An-Najah National University
Faculty of Graduate Studies

Kinetic Studies of the Hydrolysis of Furfurylidenefuroyl Hydrazone Derivatives, Solvatochromism and Fluorimetric Determination of Iron (III)

By
Mahmoud Mohammed Issa Gabaga

Under the supervision of
Prof. Bassem Shraydeh

Submitted in Partial Fulfillment of the Requirements for the Degree of Masters in Chemistry, Faculty of Graduate Studies, at An-Najah National University, Nablus, Palestine.

2005

Kinetic Studies of the Hydrolysis of Furfurylidenefuroyl Hydrazone Derivatives, Solvatochromism and Fluorimetric Determination of Iron(III)

By

Mahmoud Mohammed Issa Gabaga

This Thesis was defended successfully on 1/ 2/ 2005 and approved by:

Committee Members	Signature
1. Prof. Dr. Bassem Shraydeh (Supervisor)	
2. Dr. Nizam Diab (External examiner)	
3. Prof. Dr. Mohammed Alsubu (Internal examiner)	

To my family with all my love

Acknowledgements

First, I would like to thank my supervisor Prof. Dr.Bassem Shraydeh for his sincere encouragement, helpful, and close supervision which have been invaluable for me throughout all stages of this study.

I, also would like to thank Dr Mohamed Al-Nuri for his help in the synthesis of some hydrazones.

Also my sincere thanks go to Mahmoud Al- Shamali for his help in supplying the chemicals and reagents.

Finally I wish to thank my family for their help and encouragments.

List of Contents

List of Tables

List of Figures

Kinetic Studies of the Hydrolysis of Furfurylidenefuroyl Hydrazone Derivatives, Solvatochromism and Fluorimetric Determination of Iron (III)

By
Mahmoud Mohammed Issa Gabaga
Under the supervision of
Prof. Bassem Shraydeh

Abstract

Preferential solvation of di-2-pyridylketonebenzoyl hydrazone was investigated in aqueous-ethanol binary mixtures .

The kinetics and mechanism of the hydrolysis of a series of substituted furfurylidenefuroyl hydrazones (X-FFH) in 25% (v/v) ethanol-buffer mixtures have been studied by ultraviolet visible spectrophotometry at different temperatures in the range 22-50^{0}C. The hydrolysis reactions were found to follow first-order kinetics. The effect of pH, molecular structure and temperature on the rate of hydrolysis have been discussed.

A mechanism for the hydrolysis is postulated in which the attack of water on the protonated substrate is subject to general acid-base catalysis using HCl-sodium acetate buffer solution. The hydrolysis of 5-Chlorothiophenylidene salicoyl hydrazone (CTSH) was found to obey specific acid catalysis using HCl-KCl buffer solutions.

The observed rate constants and the catalytic rate constants with respect to H^+, $HC_2O_4^-$ and $H_2C_2O_4$ were calculated. Activation energy and thermodynamic parametres for the hydrolysis are evaluated and discussed.

A sensitive method for the determination of iron (III) in trace levels using fluorescence spectroscopy was devised. The method is based on the oxidation of di-2-pyridylketonebenzoyl hydrazone by hydrogen peroxide

whereby Fe (III) shows an inhibition effect on the emission signal. The detection limit of Fe (III) was found to be $3.0x10^{-6}$M. Interference studies and order of addition were also investigated. The method was successfully applied to milk and other medicinal samples.

Chapter One

Introduction

1.1 Hydrazones

1.2 Introduction to Spectroscopic Methods

1.3 Solvation

1.4 Kinetic Considerations

1.5 Fluorescence

1.1 Hydrazones

In chemistry, a hydrazone is a substance with the structure $R_2C=NNR_2$, differing from aldehydes or ketones by the replacement of the double bonded oxygen with the $=NNR_2$ functional group. They are formed usually by the reaction of hydrazides, hydrazines or their derivatives with ketones or aldehydes.

The hydrazone derivatives are used in clinical chemistry for the determination of some elements (Neeley, Cupas,1973; Uno, Taniguchi 1971).

1.2 Introduction to Spectroscopic Methods

The word spectroscopy is widely used to mean the separation, detection and recording of energy changes involving nuclei, atoms or molecules. These changes are due to emission, absorption or scattering of electromagnetic radiation or particles. The experimental applications of spectroscopic methods in chemical problems are diverse, but all have in common the interaction of electromagnetic radiation with the quantized energy states of matter (Henry, Gary and James 1978). When a beam of radiation is passed through an absorbing substance, the intensity of the incident radiation (I_0) will be greater than that of emergent radiation(I).

Photometric methods are perhaps the most frequently used of all spectroscopic methods and are important in quantitative analysis. The amount of visible light or other radiant energy absorbed by a solution is measured, since it depends on the concentration of the absorbing substance. In spectrophotometric methods, the ratio of the intensities of the incident and transmitted beams of light is measured at a specific wavelength by

means of detector such as a photocell. The absorption spectrum also provides a "fingerprint" for qualitatively identifying the absorbing substance (Henry, Gary and James 1978).

1.3 Solvation

The solvatochromism is the phenomenon that refers to the effect of a solvent or more to that of a molecule surrounding some spectroscopic properties of that molecule (Soukup, Schmid 1985). It is concerned with the change in position of an ultraviolet visible absorption band, accompanying a change in the polarity of the medium (Degtyarenko, et al, 1993; Yutaka, Yoshito and Tadashi, 2000). As the solvent is varied, the ground and excited state energies will vary.

If the ground and excited states interact differently with the solvent, then the difference in the excitation energy will vary with the solvent. The energy transition can be related to the frequency of light absorption through Planck equation:

$\Delta E=hc/\lambda$

h: Planck constant

c: light velocity

λ: maximum wavelength

1.3.1 Preferential solvation

The model of Frankel (Frankel, Langford and Stengle,1970) was used for the study of preferential solvation. Frankel deduced the following equation in his derivation:

$X_A/X_B=k\ (Y_A/Y_B)$

k: Preferential solvation constant

X_A, X_B: Mole fraction of solvent A and solvent B in the solvation shell

Y_A, Y_B: Mole fraction of solvent A and solvent B in bulk solvent

The plot of X_A/X_B versus Y_A/Y_B is expected to yield a straight line of slope k which represents the preferential solvation constant. The composition of the solvation shell can be determined from the intercept of the horizontal line with the diagonal line from X_A= 0 to 1.

1.4 Kinetic Considerations

1.4.1 Aquation:

The term aquation means dissociation of a complex using an acid. In the presence of acids the hydrazones dissociates to give a hydrazide and an aldehyde (Abu-Zuhri, et al 1992). The kinetics were studied under pseudo first order conditions by following the decrease of absorbance of the hydrazones at the selected wavelength at several temperatures.

1.4.2 First Order Reaction

The rate law for a reaction tells how the rate of this reaction is related to the concentrations of reactants (Mark and Lond, 1998; Ignacio, Kenneth and James, 1995). For the following example:

$A \rightarrow$ product

The rate law of this reaction takes the form :

$Rate = -d[A]/dt = k [A]^a$

If the reaction is first order, then the value of **a** equal **1**, and then the rate expression would be :

Rate = k [A].

The integrated first order rate law is:

$\ln((A_0 - A_\infty)/(A_t - A_\infty)) = kt$

Where A_0: is the absorbance at time zero, A_t: is the absorbance at time **t** and A_∞: is the absorbance at time ∞. Then a plot of $\ln(A_t - A_\infty)$ versus time will give a straight line with a slope equal to **- k**.

1.4.3 Pseudo Frst Order Reaction

Pseudo first order conditions means that to keep all concentrations of other reactants in much excess over A. If we consider the following example:

$A + B \rightarrow$ product

$-d[A]/dt = k[A]^a [B]^b$

if [B] >>> [A] then

$-d[A]/dt = k_1[A]^a$

$k_1 = k[B]^b$

Where k_1 is the pseudo first order rate constant and has units of $time^{-1}$

1.4.4 Differential Methods

Another method to prove the reaction is of the first order with respect to A is to use differential method, which is based upon the following:

$Rate = k [A]^n$

Upon taking the logarithms on both sides

$\log rate = \log k + n \log[A]$

Plotting log rate versus log [A] will give a straight line of a slope of **n**.

1.4.5 Effect of Temperature

The temperature also affects the reaction rate. The observation indicates that a rise in temperature almost invariably increases the rate of any reaction. It is known that the rate of the reaction will often double by a

10˚C rise in temperature (Ignacio, Kenneth and James 1995; Keith, John and Bryan 2003). To find the energy of activation, the Arrhenius equation usually is used

$\ln k = \ln A - E_a / RT$

k: the observed rate constant

A: Pre-exponential factor

E_a : activation Energy

R: gas constant

T: temperature (K)

Then a plot of ln k versus 1/T will be linear with a slope equal to $-E_a/R$, thus the energy of activation could be found.

1.4.6 Transition State Theory

The essential idea of this theory is based on the concept that the reaction proceeds through a transition state that is in thermodynamic equilibrium with the reactants. The overall rate of the process is then determined by the rate at which the transition state undergoes decomposition into product (Tinoco, Sauer, and Wang 1995). The thermodynamic parameters were evaluated using the transition state theory equations.

The participation of the transition state can be represented as follows:

$A + B \rightarrow AB \rightarrow$ product

The final desired form is:

$$k = RT/Nh \exp(-\Delta G^{\neq}/RT) \quad (1)$$

$$k = RT/Nh \exp(-\Delta S^{\neq}/R) \exp(-\Delta H^{\neq}/RT) \quad (2)$$

While $\Delta H^{\neq} = E_a - nRT$ (3)

And $k_b = R/N$ (4)

In solutions and in unimolecular reactions this equation becomes:

$k = k_b T/h \exp(1+\Delta S^{\neq}/R) \exp(- E_a /RT)$ (5)

where k: the observed rate constant.

k_b: the Boltzman constant.

T: the absolute temperature

$\Delta S^{\neq}$: the entropy of activation.

E_a: energy of activation

h : Planck constant

The entropy of activation gives a useful indication of the structure of the transition state. A positive entropy of activation indicates that the transition state is less ordered than the individual reactant molecules, while a negative entropy of activation corresponds to an increase in order of the transition state.

1.4.7 Specific and General Acid-base Catalysis

Specific and general acid base catalysis have been extensively studied on various hydrazones (Abobakr El-Nady, 2001; Abu-Eid, et al 1989; Abu-Zuhri, et al 1992; Keith, John and Bryan. 2003; Ewa., David and Anthony 2000).

In specific acid-base catalysis the rate of reaction is proportional only to the concentration of H^+. This implication means that the catalytic constant

of the hydrogen ion is much larger than that of the other acids and bases in the reaction (Laidler, Meiser and Sanctuary, 2003; Ewa, David. and

Anthony 2000). The following equation is obeyed with respect to acid catalysis:

$$\log k_{obs} = \log k_{H^+} - pH$$

It will be seen that a plot of log k_{obs} against pH will give a straight line of a slope equal –1.00. Similary in specific base catalysis a reaction only is catalysed by OH^-. The relevant equation is:

$$\log k_{obs} = \log k_{OH^-} + \log k_W + pH$$

It will be seen that a plot of log k_{obs} against pH will give a straight line of a slope equal 1.00.

Whereas the general acid-base catalysis involves a reversible reaction between a substrate molecule S and an acid or base molecule (Keith, John and Bryan 2003):

$$S + HA \rightarrow SH^+ + A^-$$

$$SH^+ + H_2O \rightarrow \text{product}$$

Assuming that the uncatalysed reaction makes a negligible contribution to the rate, then the following equation is obeyed with respect to general acid catalysis.

$$k_{cat} = k_{H^+}[H^+] + k_{HA}[HA] + k_{A^-}[A^-]$$

The reaction is studied at two different pH values where $[HA]/[A^-]$ is a constant, say x_1 and x_2 respectively.

Under these conditions the above equation can be represented by

$k_{cat} = k_H^+[H^+] + k_{HA}[HA] + k_A^-[HA]/x_1$ and

$k_{cat} = k_H^+[H^+] + k_{HA}[HA] + k_A^-[HA]/x_2$

A plot of k_{cat} against [HA] for solutions buffered with $[HA]/[A^{-1}]$ ratios of x_1 and x_2 gives a straight lines with slopes equal to $k_{HA} + k_A^{-1}/x_1$ and $k_{HA} + k_A^{-1}/x_2$ respectively from which the values of k_{HA} and k_A^{-1} are determined.

1.5 Fluorescence

The four main components of any fluorescence instrument are the source of excitation, the sample cell, the detector and the filters or gratings used to select the exciting and emitted radiation (Henry, Gary and James, 1978).

Fluorescence is the emission of light from a molecule in which an electronically excited state has been populated (Robert 1983; George 1990). The emission of light is usually in the ultra violet to visible portion of the spectrum. The absorption is the process that an electron is raised from the ground state to an excited state which leads to fluorescence usually involves a (π to $\pi^{\#}$) electronic transition in an organic molecule. Transition can occur into various vibrational levels of the excited electronic state, depending upon the exact energies of the absorbed photons.

Any fluorescent molecule has two characteristic spectra: the excitation spectrum and the emission spectrum (Lin, et al 1995). In conventional fluorimetry, the fluorescence intensity is recorded as a function of the emission wavelength while the excitation wavelength is held at a constant value. Excitation fluorimetry involves the reverse situation that is the

variation of the excitation wavelength at a constant emission wavelength Roberts, Lloyd and Clarke 2002.

The excitation spectrum obtained with a fluorimeter, should be identical with the absorption spectrum of the molecule, obtained with a spectrofluorimeter. The emission spectrum of a compound results from the re-emission of radiation absorbed by that molecule. If the exciting radiation is at a wavelength that differs from the wavelength of the absorption peak, less radiant energy will be absorbed and less will be emitted (Hering and Morel 1990).

There are many factors that affect the fluorescence intensity:

1-The quantum efficiency: the ratio of the total energy emitted by any molecule per quantum of energy absorbed.

2-The intensity of incident radiation. As the intensity of incident light increases fluorescence intensity increases

3-The molar absorptivity of the compound.

4-The concentration of fluorescent molecules.

5- The temperature.

Fluorescence spectroscopy has become a major movement within the fields of biophysics, medical science and analytical chemistry (Oshite, Furukawa and Igarashi, 2001; Nevado.J.J.B, Pulgarh.J.A.M and Laguna, 1998). In the limited reports available on kinetics, excitation or emission spectra have been used to study the kinetics of fluorescence quenching or enhancement when a molecule binds with metals, e.g Cu, Fe and Al

(Jinzhang, et al 2003; Ren, et al 2001; Wuilloud, Wuilloud, Olsina and Martenez, 2001; Karvinen, et al, 2004).

Ideally the relation between the concentration of the fluorescence molecules in solution and the emitted radiant power would be linear.

$P_{em}= kC$

P_{em} : emitted power

k : constant

C : concentration

Fluorescent analysis is widely used also as a detection technique in diagnostics, drug screening and monitoring of drug delivery due to its minimal effect on the sample (Roberts, Lloyd and Clarke 2002). Fluorescence spectroscopy is well known as a sensitive, accurate and

convenient analytical tool and has been applied to the analysis of various fluorescent labelled molecules in solutions and in much more complex systems (Rubio, Gomez-Hens and Valcarcel 2001).

It was established in the literature the use of various hydrazones for spectrofluorimetric determination of elements (Uno, Taniguchi 1971). On the other hand Ce(VI), $KBrO_3$ and sodium perborate were employed as oxdizing agent (Khashaba 2002; Shoeb, Bowman, Ottolenghi and Merola, 1985; Kurokawa, Maekawa, Takahabashi and Hayashi, 2001).

1.6 Stoichiometric Studies of the Complex

There are different methods used to determine the formula of the complex. The well known method is molar-ratio. This method can be followed by spectrofluorimetric or spectrophotometric techniques.

1.7 Ligands and Their Structures

Di-2- pyridyl Ketone Benzoyl Hydrazone (DPKBH):

It is a heterocyclic hydrazone which contains nitrogen. Its structure is:

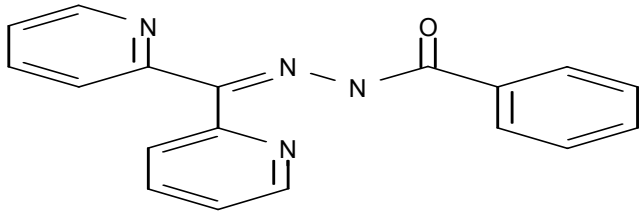

5- Chlorothiophenylidene Salicoyl Hydrazone (CTSH):

It is a heterocyclic hydrazone which contains sulfur. Its structure is:

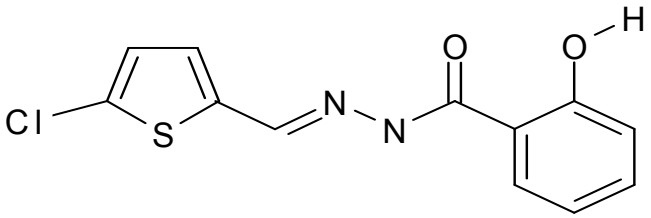

2- Furfurylidene 2-Furoyl Hydrazone(FFH):

It is a heterocyclic hydrazone which contains oxygen. Its structure is:

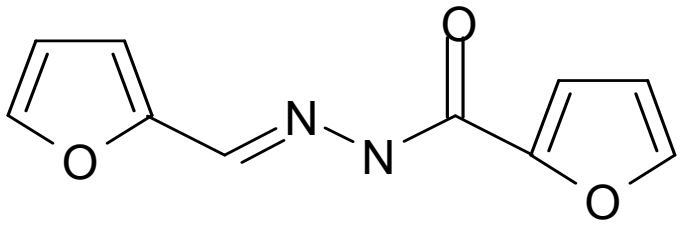

5- Bromo-Furfurylidene Furoyl Hydrazone(BFFH):

It is a heterocyclic hydrazone which contains oxygen. Its structure is :

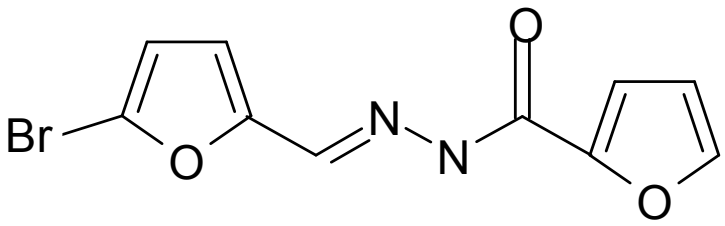

5- Methyl-Furfurylidene Furoyl Hydrazone(5-Methyl-FFH):

It is a heterocyclic hydrazone which contains oxygen. Its structure is :

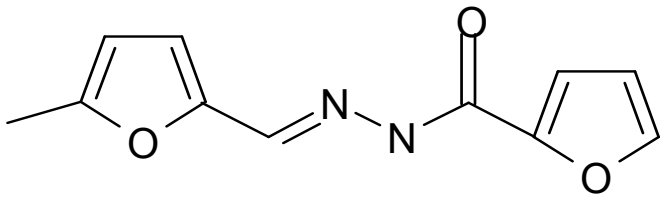

5- Nitro-Furfurylidene Furoyl Hydrazone(5-Nitro-FFH):

It is a heterocyclic hydrazone which contains oxygen. Its structure is :

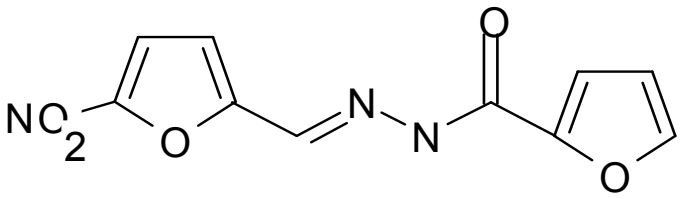

The Purpose of this Study

The present research aimed to :

1- Investigate preferential solvation of DPKBH in ethanol-aqueous binary solvent.

2- Determinate of Fe(III) concentrations in milk and medicine samples using fluorescence spectroscopy.

3- Investigate the Arrhenius parameters for aquation of some hydrazone derivatives and the effect of the substituent on the rate of hydrolysis of these hydrazones.

Chapter Two

Experimental

2.1 Instrumentation

Solvation and kinetic runs for the hydrolysis of some hydrazones were spectrophotometrically performed using ultraviolet visible spectrophotometer (Shimadzu) equiped with 1-cm quartz cells and kinetic facilities.

A perkin-Elmer Luminescence spectrometer (LS 50B), 1-cm quartz cells, and a water bath circulator were employed for the fluorescence measurements.

The spectrofluorimeter is fitted with a device for kinetic measurements, that permits direct recording of fluorescence-time graphs at fixed excitation and emission wavelengths. All measurements were recorded with the following condition: emission and excitation slit width of 6 nm.

All pH measurements were carried out using a corning pH-meter. Infrared spectra were made using Fourier Transform Infrared spectrometer model (8201 PC) (FTIR) Shimadzu.

2.2 Materials

All chemical used in this work were obtained from Merck: 2-furoic acid hydrazide, 2-furaldehyde, 5-methyl-2-furaldehyde, 5-bromo-2-furaldehyde, 5-nitro-2- furaldehyde, di-2-pyridyl ketone and benzoic acid hydrazide.

35%(v/v) Hydrogen peroxide solution, concentrated hydrochloric acid. Buffers used as hydrolysis media: hydrochloric acid-potassium chloride buffer series, hydrochloric acid-sodium acetate buffer series and

oxalic acid-potassium oxalate buffer series were prepared and used as hydrolysis media.

2.3 Solvatochromic Measurements

Solvatochromic measurement were performed using a minute crystal of DPKBH in various mole fractions of ethanol-aqueous solution. The solute was added to a 1-cm quartz cell to yield an absorbance of nearly unity. Then the spectra was run, and the wavelength of maximum absorption was recorded.

2.4 Kinetic Measurements

Reactions were perfomed by mixing 3.0 ml of the buffer solutions, and 1.0 ml of 40 ppm hydrazone solutions (CTSH, FFH) at a fixed temperature. The mixture was shaken and transferred to the 1-cm cell, and the change in absorbance with time was recorded at the selected wavelength.

The wavelengths selected in the rate studies of (CTSH, FFH, 5-nitro-FFH, 5-methyl-FFH and 5-bromo) were 324 nm, 371 nm, 372 nm, 331nm, 331nm, respectively.

2.5 Fluorimetric Measurements

The following solutions were mixed in the following order 1-ml of Fe(III) solutions, 1-ml of DPKBH, 2-ml of concentrated hydrochloric acid and 1ml of 35%(v/v) hydrogen peroxide solutions. A portion of this solution was transferred rapidly to the spectrofluorimeter quartz cell. The reaction was monitored by recording the intensity of the emitted fluorescence versus time at an emission wavelength of 431nm, and an excitation

wavelength of 375 nm with a slit width of 6 nm.. The fixed time method was used whereby the fluorescent intensity is measured after 50 s. The initial rate was calculated from the slope of the fluorescence intensity of the emitted fluorescence light versus time.

2.6 Preparation of Hydrazones

Di-2-pyridylketonebenzoyl hydrazone (DPKBH) prepared by reaction of di-2-pyridyl ketone (2.359g) and benzoic acid hydrazide (2.000g) in stoichiometric amounts. The mixture is heated at reflux for four hours, using absolute ethanol. During this period the colour of solution changes. The product was recrystallized from ethanol to constant melting point (130-135ºC). 5-Methyl -2- furfurylidene -2- furoyl hydrazone (5-Methyl-FFH) was prepared by reaction of 5-methy l-2-fural (1.976) and 2-furoic acid hydrazide (2.000g) in stoichiometric amounts. The mixture is heated at reflux for four hours, using absolute ethanol. During this period the colour of solution changes. The product was recrystallized from ethanol to constant melting point (160-163ºC). 5-Nitro-2-furfurylidene -2-furoyl hydrazone (5-Nitro-FFH) was prepared by reaction of 5-nitro-2-fural (2.240g) and 2-furoic acid hydrazide (2.000g) in stoichiometric amounts. The mixture is heated at reflux for four hours, using absolute ethanol. During this period the colour of solution changes. The product was recrystallized from ethanol to constant melting point (259-261ºC).

5-Bromo-2-furfurylidene-2-furoyl hydrazone (5-Bromo-FFH) was prepared by reaction of 5-bromo-2-fural (2.777g) and 2-furoic acid hydrazide (2.000g) in stoichiometric amounts. The mixture is heated at reflux for four hours, using absolute ethanol. During this period the colour of solution changes. The product was recrystallized from ethanol to

constant melting point (182-185ºC). Boiling stones are added during heating to ensure smooth boiling. At this stage, any material which does not dissolve will be removed by hot filtration. The hot solution is allowed to cool slowly and crystals of the desired material form, while the impurities remain in solvent. The crystals are collected by suction filtration

Chapter Three

Results And Discussions

Part A: Solvatochromism

Part B: Kinetics

Part C: Fluorescence

Part A: Solvation

The solvatochromism studied in this work belongs to the solvatochromic probe di-2-pyridylketonebenzoyl hydrazone. All of the work was performed using various mole fraction of ethanol-water solutions.

Table A1 lists the wavelength, wave number and mole fraction of the organic solvent. This table shows clearly that with increasing mole fraction of ethanol solvent the energy decreases.

In the plots of energy versus mole fraction of ethanol there is a deviation from linearity, this indicates that there is a preferential solvation. The model of Frankel was used in analysis of the results. The plots of transfer energies versus bulk solvent composition of the complexes reflect the solvation shell instead of the bulk solvent composition.

For a given solvent composition X_A, the measured frequency corresponds to an effective concentration Y_A to be determined at the intercept of the horizontal line with the diagonal straight line ($X_A = 0 \rightarrow X_A = 1$). These tie lines are manifested in FigaerA1.

Table A1. Wavelength(λ_{max}) and wave numbers of maximum absorption (cm^{-1}) for the lowest energy transfer bond of di-2-pyridyl ketone benzoyl hydrazone at various mole fraction of ethanol at room temperature (298.15K).

λ_{max} (nm)	$Y_{ethanol}$(v/v)	10^3. wave number (cm^{-1})
315.5	0.0	3.170
321.0	0.1	3.115
323.0	0.2	3.096
325.0	0.3	3.077
327.5	0.4	3.053
329.0	0.5	3.049
330.0	0.6	3.030

λ_{max} (nm)	$Y_{ethanol}$(v/v)	10^3. wave number (cm^{-1})
332.0	0.7	3.012
332.5	0.8	3.008
333.0	0.9	3.003
334.5	1.0	2.990

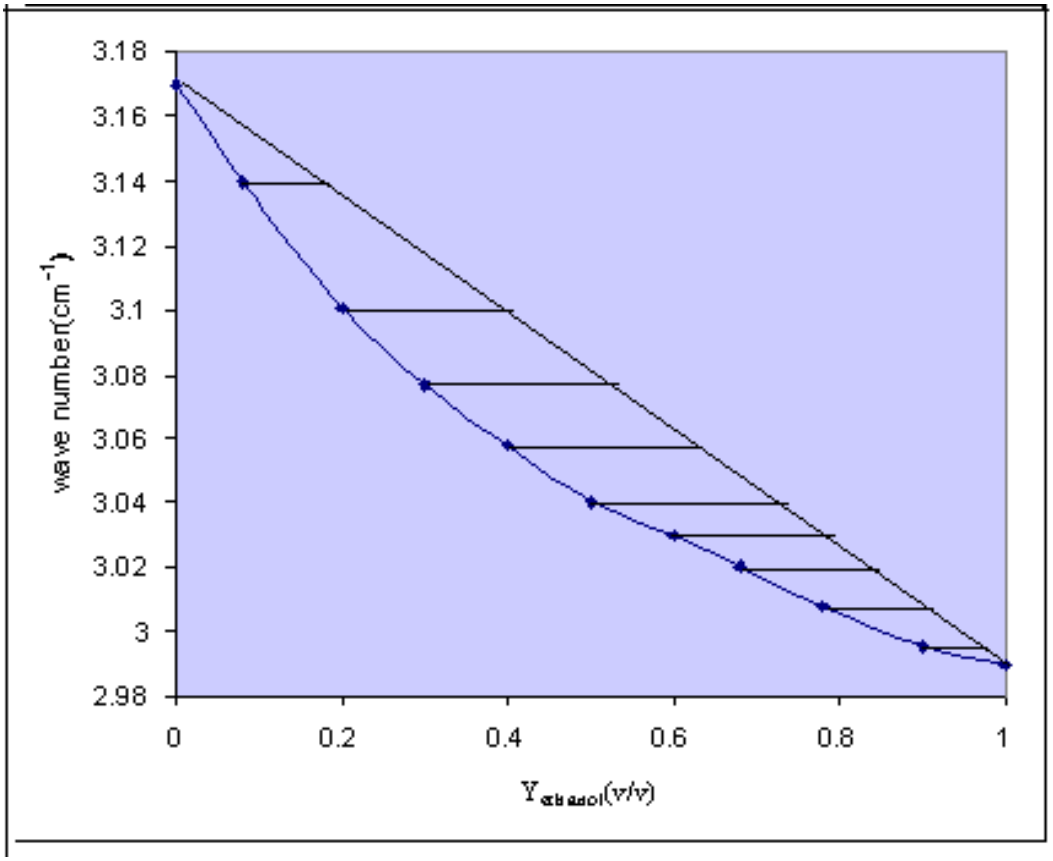

Figaer A1. Tie lines construction from the frequency plots for equilibrium between bulk and solvation phases at 298.15K for di-2-pyridylketone benzoyl hydrazone in the ethanol -water system.

Table A2 lists the ratio of mole fractons of bulk (Y) and solvation (X) phases at equilibrium at 298.15K for the solvatochromic behavior of DPKBH in binary ethanol-water systems. As for example: $Y_{ethanol}$ = 0.27 then Y_{water} = 1 - 0.27 = 0.73 and from the tie line $X_{ethanol}$ = 0.53 then X_{water} = 1-0.53 = 0.47

According to the model described by Frankel, the plots X_A/X_B versus Y_A/Y_B is expected to be linear, as is found experimentally Figaer

A2. The preferential solvation constant which is found from this linear plot is 3.07 however the value of the preferential solvation constant is low suggested that solvation phenomena is not sufficient too.

It is then observed as manifested in Table A1 that as the fraction of ethanol solvent increases then the energy decreases. In this case the ground-state solvation results from dipole-dipole forces, there is an oriented solvent cage a round the dipolar solute (DPKBH) molecules, resulting in a net stabilization of the ground state of the DPKBH. Thus, with increasing the ethanol percentage the energy of the ground state is lowered less than that of the excited state and this produces a hypsochromic shift. The dipolar DPKBH molecules cause an electronic polarization of the surrounding solvent molecules. For solvatochromic compounds the observed solvent induced wavelength shifts can be explained in terms of a change in the permanent dipole moment on electronic transition ($\mu_g \neq \mu_e$). The change in ground state dipole moment of the solute, induced by the surrounding solvent cage must also be taken into account. The dipolar solute molecules cause an electronic polarization of the surrounding solvent molecules.

Table A2. Ratio of mole fraction of bulk (Y) and solvation (X) phases at equilibrium at 298.15 ^{0}K for the solvatochromic behavior of di-2-pyridyl ketone benzoyl hydrazone in the binary ethanol-water system.

Y_{eth}/Y_{water}	Y_{water}	$Y_{ethanol}$	X_{eth}/X_{water}	X_{water}	$X_{ethanol}$
0.04	0.127	0.89	0.11	0.042	0.96
0.06	0.209	0.83	0.17	0.064	0.94
0.12	0.429	0.70	0.30	0.137	0.88
0.20	0.695	0.59	0.41	0.250	0.80

Y_{eth}/Y_{water}	Y_{water}	$Y_{ethanol}$	X_{eth}/X_{water}	X_{water}	$X_{ethanol}$
0.27	1.128	0.47	0.53	0.362	0.73
0.31	1.421	0.41	0.59	0.456	0.69
0.38	1.857	0.35	0.65	0.613	0.62
0.45	2.333	0.30	0.70	0.818	0.55
0.53	3.274	0.23	0.77	1.141	0.47
0.63	4.556	0.18	0.82	1.703	0.37
0.67	6.143	0.14	0.86	2.003	0.33
0.72	7.696	0.11	0.89	2.509	0.28
0.83	11.500	0.08	0.92	4.714	0.17

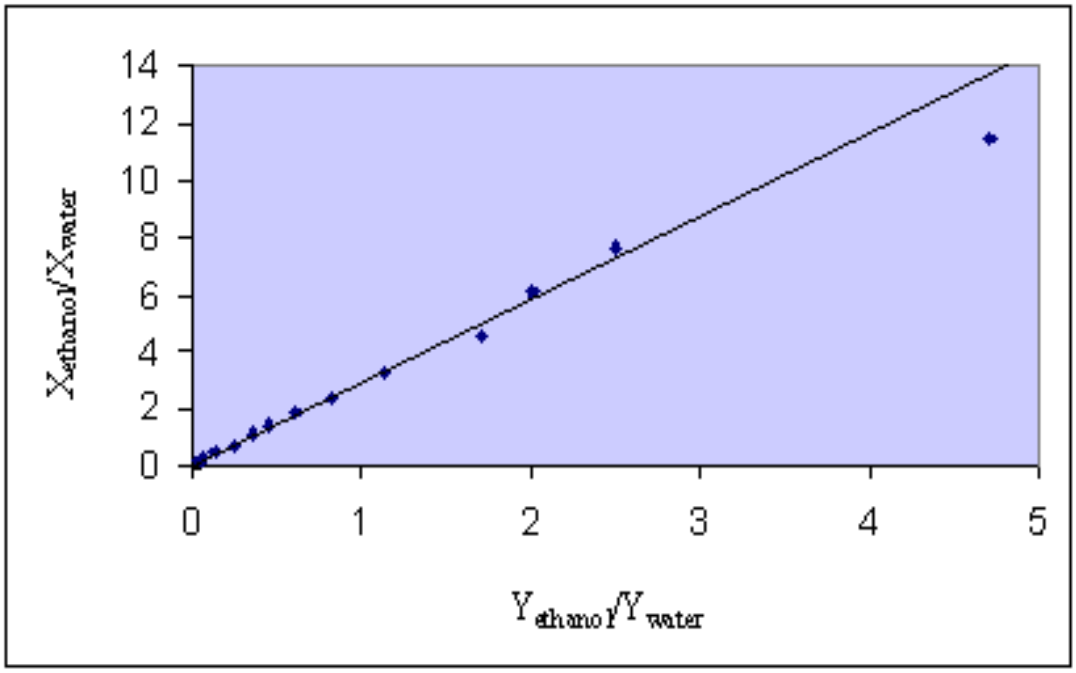

Figaer A2. Preferential solvation plot ($X_{ethanol}/X_{water)}$ against ($Y_{ethanol}/Y_{water}$) for di-2-pyridylketone benzoyl hydrazone at 298.15ºK in ethanol-water system.

The slope of the plot (preferential solvation constant) is equal to 3.07

Part B: Kinetics

The hydrolysis of 5-Chlorothiophenylidenesalicoyl hydrazone, and 2-Furfurylidenefuroyl hydrazone derivatives in aqueous medium containing 25% ethanol have been found to follow first order kinetics similar to that previously reported for the hydrolysis of furfurylidene benzoyl hydrazone (FBH), pyrrolidene benzoyl hydrazone (PBH) and thiophenylidene benzoyl hydrazone (TBH) (Abu-Zuhri, Abu-Eid, Al-Nuri and Mahmoud, 1992).

It was observed that the rates of hydrolysis of these compounds above pH 2.0 were very slow. Therefore, the rates of the hydrolysis reactions were studied using buffer in the pH range (less than 2.0).

Kinetic Hydrolysis of 5-Chlorothiophenylidenesalicoyl Hydrazone (CTSH)

Straight lines were obtained by plotting $\ln(A_t-A_\infty)$ versus time for the hydrolysis of 5- Chlorothiophenylidene salicoyl hydrazone CTSH. The rate constants for these reactions were determined from the linear plots of $\ln(A_t-A_\infty)$ versus time. A typical plot is manifested in FigaerB1.

The effect of temperature is manifested in Table B1. It can be shown that the rate constants generally increase upon increase of temperature. The Arrhenius plot is linear and is shown in FigaerB2. The Arrhenius parameters for the hydrolysis of (CTSH) hydrazone is evaluated using the transition state theory equations.

It was found that the observed rate constant increased gradually on decreasing the pH value as shown in Table B3. A straight line was

obtained by plotting log k_{obs} versus pH for the hydrolysis of 5-Chlorothiophenylidenesalicoyl hydrazone (CTSH) (FigaerB3), using hydrochloric acid-potassium chloride buffers as the hydrolysis medium at room temperature 298.15K. The slope of such line is found to be unity, which indicates a specific acid catalyzed mechanism.

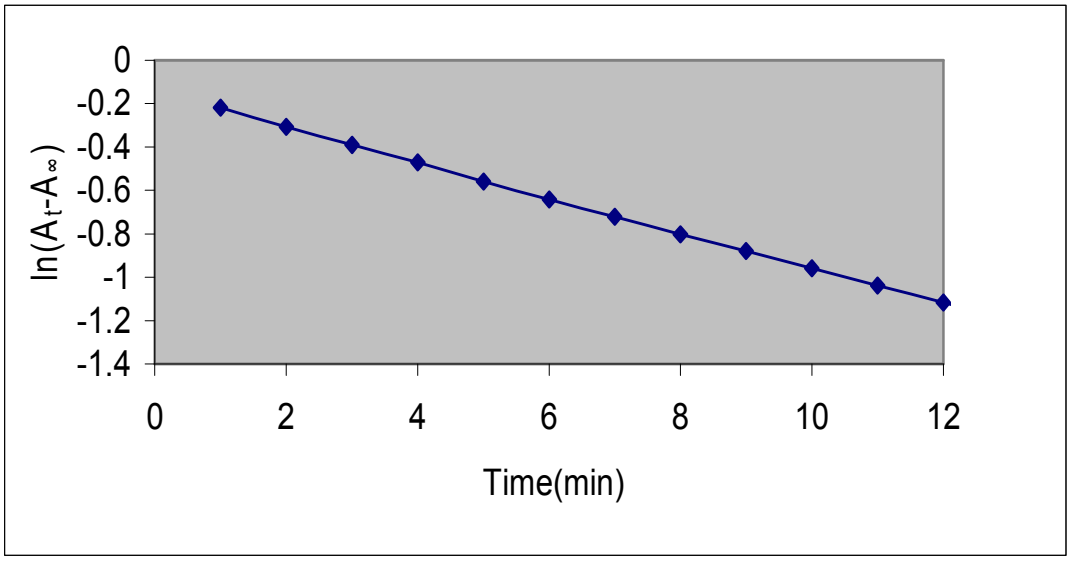

Figaer B1. A first order plot of $\ln(A_t-A_\infty)$ versus time for aquation of (CTSH), 40 ppm in 25% by volume ethanol at pH =1.0, and at room temperature 298.15 K.

Table B1. Effect of temperature on rate constants for the hydrolysis of CTSH at pH = 1.0

Temp (K)	**10^3. 1/T.(K^{-1})**	**$10^3.k_{obs}.\ s^{-1}$**	**log k_{obs}**
298.15	3.354	2.42	-2.62
303.15	3.299	2.70	-2.57
308.15	3.245	3.02	-2.52
312.15	3.204	3.29	-2.48
317.15	3.153	3.70	-2.43
-2.41	320.15	3.124	3.88

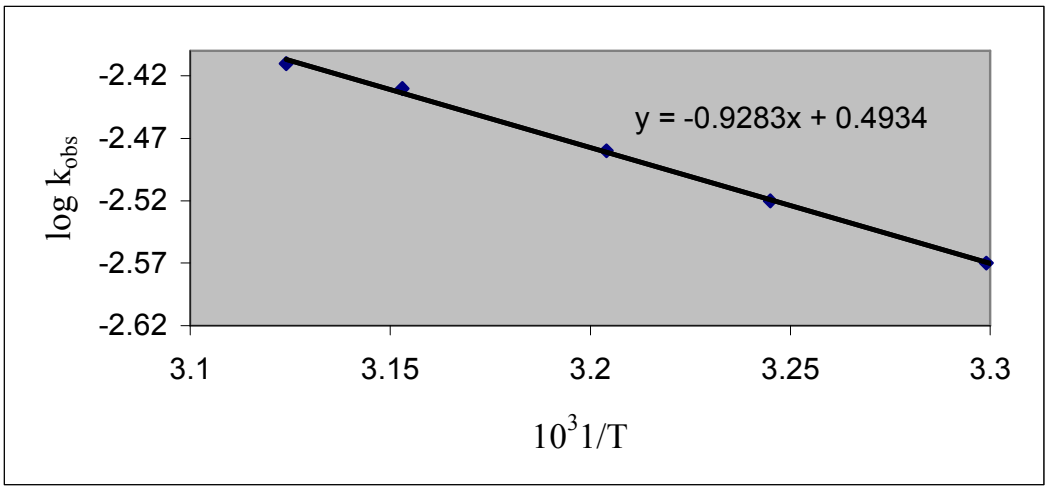

Figaer B2. Arrhenius plot for the aquation of CTSH in 25% by volume ethanol.

Table B2. Arrhenius parameters for the hydrolysis of CTSH at room temperature 298.15K and pH =1.0

Compound	**$10^3 \cdot k_{obs} s^{-1}$**	**E_a kJ/mol**	**$\Delta H^{\neq}$ kJ/mol**	**$\Delta G^{\neq}$ kJ/mol**	**$\Delta S^{\neq}$ J/mol.K**
CTSH	2.23	17.81	15.33	86.21	-241.26

Table B3. Average first order rate constants at different pH values for the aquation of CTSH in acidic medium at room temperature(298.15K)

pH	**10^3 k_{obs}. s^{-1}**	**log (k_{obs})**
1.00	2.42	-2.62
1.12	2.34	-2.64
1.22	2.00	-2.70
1.45	1.05	-2.98
1.70	0.41	-3.39
1.89	0.33	-3.48
2.11	0.19	-3.73

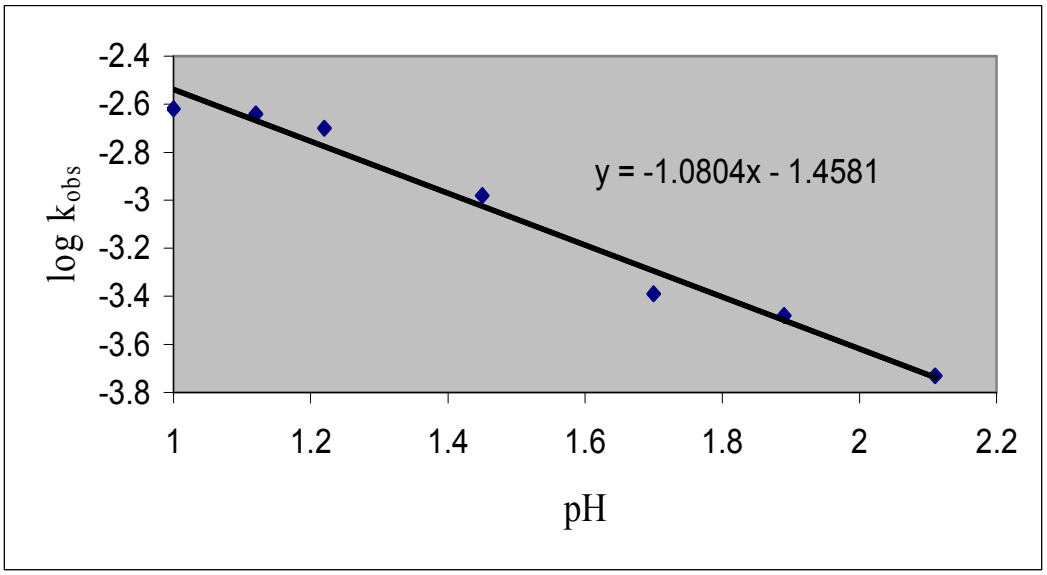

Figaer B3. A plot of log k_{obs} versus pH for aquation of CTSH in 25% ethanol(v/v) at room temperature

The mechanism of the reaction

From the above results the following mechanism is postulated.. Therefore the mechanism of the hydrolysis could be written as follows:

$$\underset{\text{(I)}}{\text{Ar-CH=N-NH(CO)Ar}} + H^{+} \underset{k_{-1}}{\overset{k_{1}}{\rightleftharpoons}} \underset{\text{(II)}}{\text{Ar-CH=}\overset{+}{\text{N}}\text{H-NH(CO)Ar}} \qquad (1)$$

$$\text{(II)} + H_2O \xrightarrow[\text{slow}]{k_2} \underset{\text{(III)}}{\text{Ar-CH(OH)-NH-NH(CO)Ar}} + H^{+} \qquad (2)$$

$$\text{(III)} \xrightarrow{k_3} \underset{\text{(IV)}}{\text{Ar-CH(O}^{-}\text{)-}\overset{+}{\text{N}}\text{H}_2} + \text{NH(CO)Ar} \qquad (3)$$

$$\text{(IV)} \xrightarrow{k_4} \text{Ar(CO)H} + \text{NH}_2\text{NH(CO)Ar} \qquad (4)$$

The rate of the reaction is the rate of the slowest step (step 2). Therfore,

Rate = k_2 [II] where II is the protonated hydrazone

From step 1 K= k_1/k_{-1} =[II]/[I][H^+] then

[II] = K[I][H^+]

Substituting the value of II gives

Rate = k_2 K[I] [H^+]

Since [H^+] is acatalyst and its concentration is high and constant denoted by C**,** then

Rate = k_2 K C[I] = k [I]

Where k is the pseudo first order rate constant and equal to

k = k_2 K [H^+]

This mechanism agrees with the experimental findings as seen above.

Kinetics of hydrolysis of 2-furfurylidenefuroyl hydrazone (FFH):

derevatives

Straight lines were obtained by plotting ln(A_t-A_∞) versus time for the hydrolysis of all X-FFH derivatives. The rate constants for these reactions were determined from the linear plots of ln(A_t-A_∞) versus time. These plots are manifested in Figures B(4-8).

The effect of temperature is manifested in Tables B(4-7). It can be shown that the rate constants generally increase upon increase of

temperature. The Arrhenius plots are linear and are shown in Figures B(9-13). The Arrhenius parameters for the hydrolysis of (X-FFH) hydrazone derivatives are evaluated using the transition state theory equations as described above. These parameters are listed in Table B8.

It was found that the observed rate constant increase gradually upon decrease of pH value as shown in Tables B(9-12). A typical plot which shows the variation of the rate versus pH for 5-methyl-FFH is shown in FigaerB14, which shows exclusively that the rate increases upon decreases of pH. A straight lines were obtained by plotting log k_{obs} versus pH for the hydrolysis of X-FFH derivatives, using hydrochloric acid-sodium acetate buffers as the hydrolysis medium at room temperature 298.15K as manifested in Figures B(15-19). The slopes of these lines are not unity which indicate a general acid catalyzed mechanism. To confirm that the mechanism is of the type general acid-base catalysis it is necessary to perform runs to show that the rate constants increase linearly upon increase of the anion concentration. For this purpose the hydrolysis of 5-methyl-FFH and 5-bromo-FFH are studied using potassium hydrogen tetraoxalate oxalic acid buffers as a hydrolysis medium. At constant pH value, the ratio of an acid to anion was held constant and the ionic strength was maintained constant at (0.10) by addition of KCl while the total concentration of the buffers was changed.

Table B13 shows the effects of anion concentration at a fixed pH on the observed rate constants for the hydrolysis of FFH derivatives. It can be seen that the observed rate constants increase linearly with increasing the anion concentration, which confirms a general acid-base catalysis mechanism for the hydrolysis of all FFH derivatives).

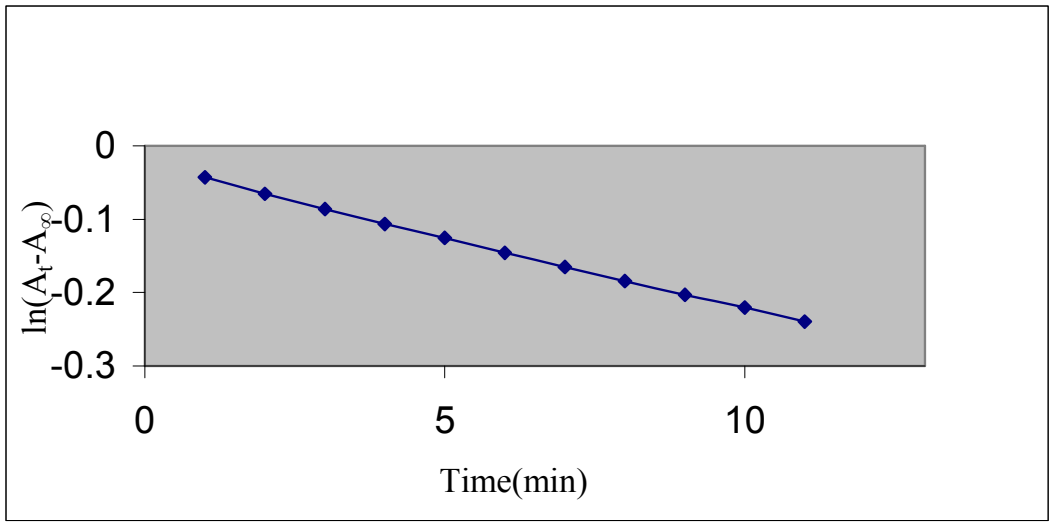

Figaer B4. A first order plot of ln(At-A∞) versus time for aquation of 40 ppm (FFH), in 25% by volume ethanol at pH (1.27), and at room temperature(298.15K**)**

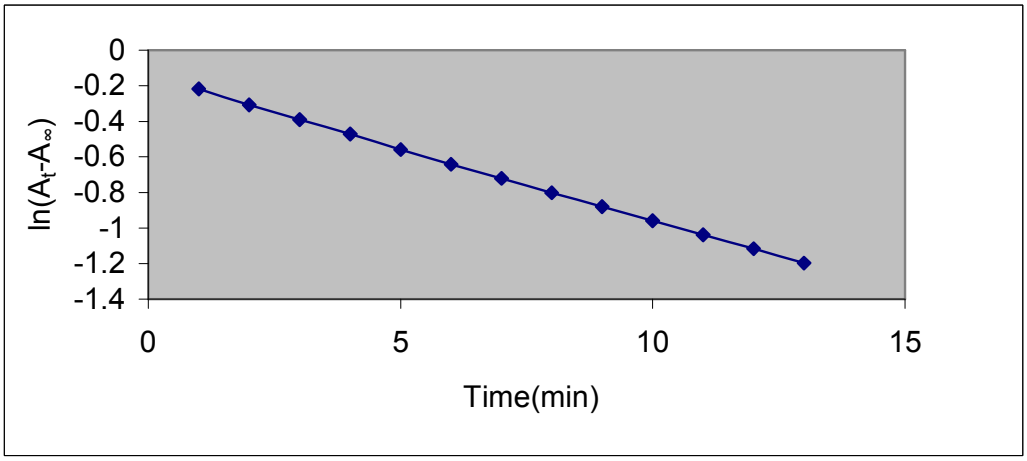

Figaer B5. A first order plot of ln (At-A∞) versus time for aquation of 40 ppm 5-methyl-FFH in 25% by volume ethanol at pH (1.1), and at room temperature (298.15 K).

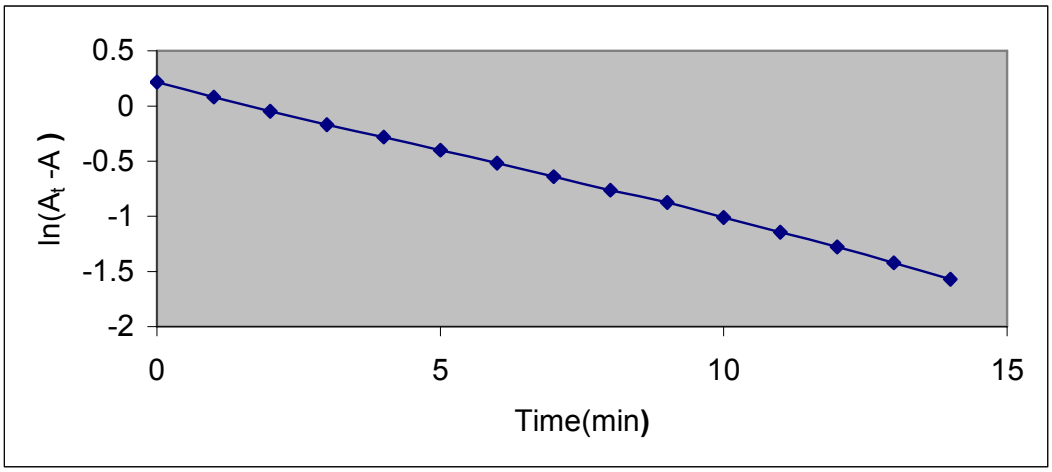

Figaer B6. A first order plot of ln(At-A∞) versus time for aquation of 40 ppm 5-nitro-FFH) in 25% by volume ethanol at pH (0.94), and at room temperature (298.15K).

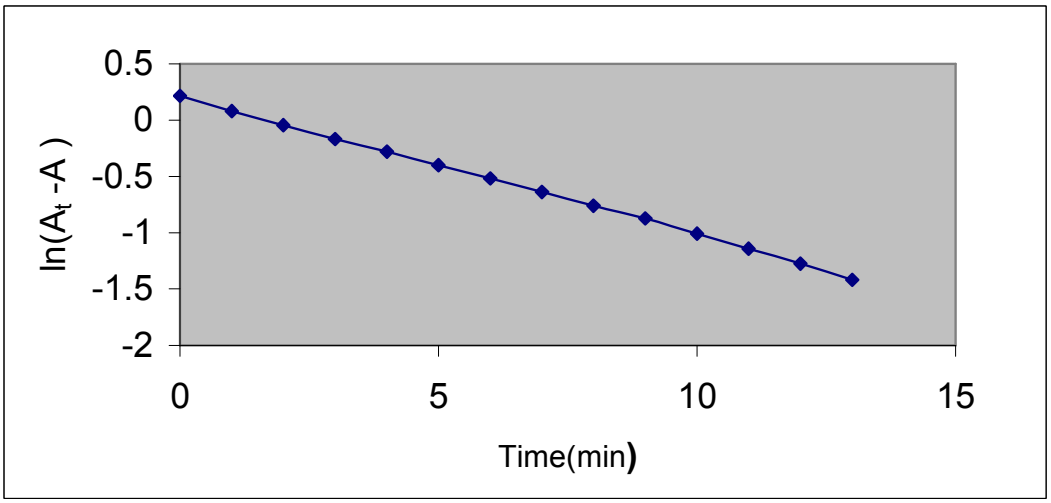

Figaer B7. A first order plot of ln(At-A∞) versus time for aquation of 40 ppm 5-bromo-FFH in 25% by volume ethanol at pH (1.0), and at room temperature (298.15K).

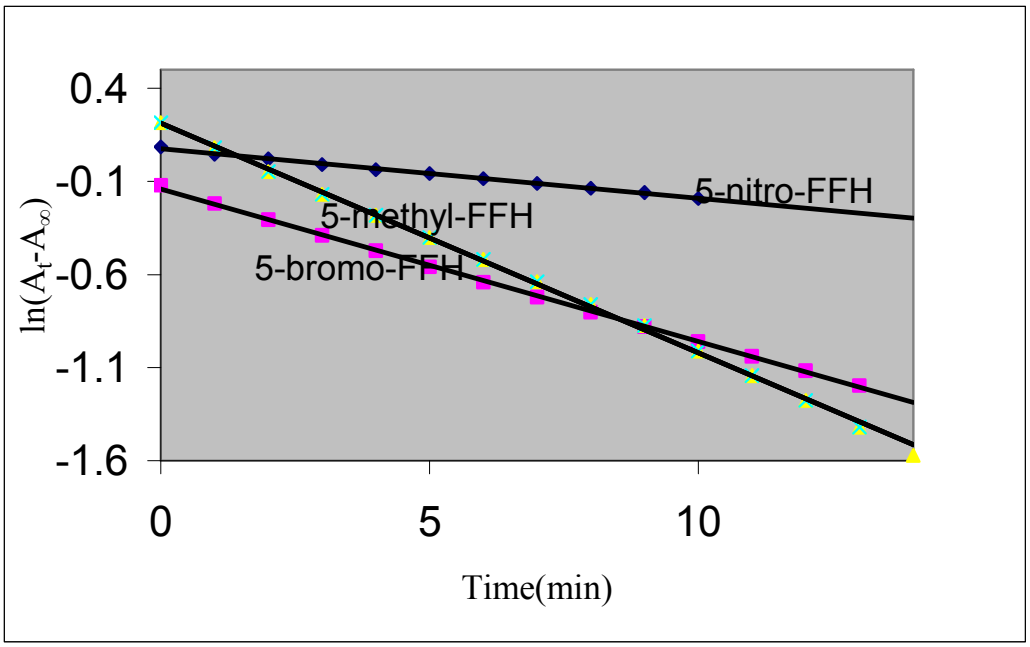

Figaer B8. A first order plot of ln(At-A∞) versus time for aquation of 40 ppm FFH derivatives in 25% by volume ethanol at pH (5-methyl-FFH=1.10, 5-bromo-FFH= 1.00 and 5-nitro-FFH=0.94) and at room temperature (298.15K).

Table B4. Effect of temperature on the hydrolysis of FFH at pH=1.00

Temp (K)	**$10^3.k_{obs}.\ s^{-1}$**	**$10^3.\ 1/T.(K^{-1})$**	**log k_{obs}**
298.15	3.354	2.10	-2.68
303.15	3.299	2.13	-2.67
308.15	3.245	2.50	-2.60
310.15	3.220	2.67	-2.57
313.15	3.192	2.95	-2.53
318.15	3.141	3.11	-2.51
323.15	3.092	3.26	-2.49

Table B5. Effect of temperature on the hydrolysis of 5-bromo-FFH at pH =1.00

Temp (K)	**10^3. 1/T.(K^{-1})**	**$10^3.k_{obs}$. s^{-1}**	**k_{obs}**
295.15	3.390	1.67	-2.78
298.15	3.354	1.80	-2.75
301.15	3.323	1.85	-2.73
303.15	3.299	1.91	-2.72
308.15	3.245	2.05	-2.69
313.15	3.192	2.22	-2.65
323.15	3.092	2.50	-2.60

Table B6. Effect of temperature on the hydrolysis of 5-methyl-FFH at pH=1.00

$10^3.k_{obs}$. s^{-1}	10^3. 1/T.(K^{-1})	Temp (K)	log k_{obs}
295.15	3.390	2.51	-2.60
298.15	3.354	2.63	-2.58
303.15	3.299	3.08	-2.51
308.15	3.245	3.13	-2.51
310.15	3.220	3.19	-2.50
318.15	3.141	3.33	-2.48
323.15	3.092	3.56	-2.44

Table B7. Effect of temperature on the hydrolysis of 5-nitro-FFH at pH=1.00

Temp (K)	10^3. 1/T.(K^{-1})	$10^3.k_{obs}.\ s^{-1}$	log k_{obs}
295.15	3.390	0.95	-3.02
298.15	3.354	0.97	-3.01
303.15	3.299	1.17	-2.93
308.15	3.245	1.32	-2.88
313.15	3.192	1.58	-2.80
326.15	3.071	1.67	-2.78
328.15	3.042	1.71	-2.77

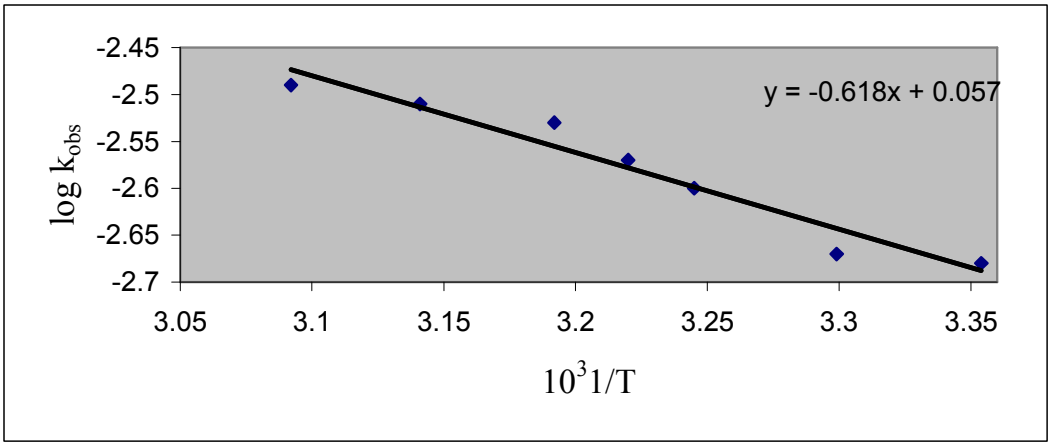

Figaer B9. Arrhenius plot for the aquation of FFH in 25% by volume ethanol

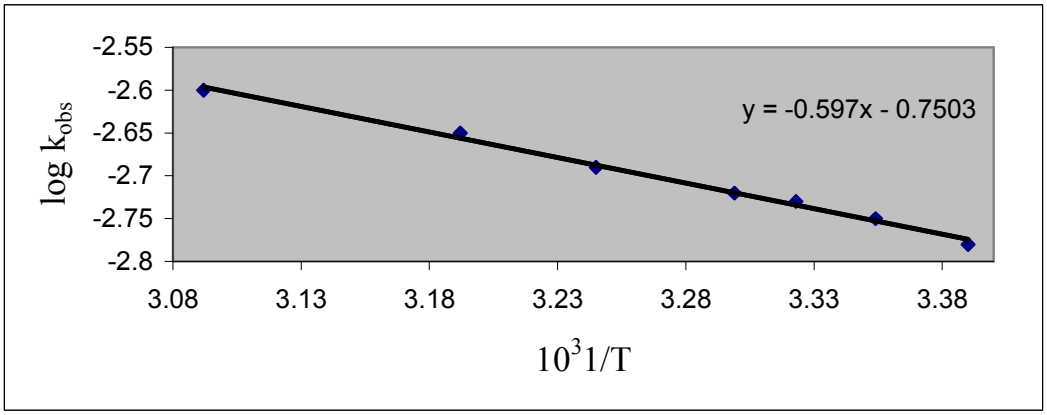

Figaer B10. Arrhenius plot for the aquation of 5-Bromo-FFH in 25% by volume ethanol.

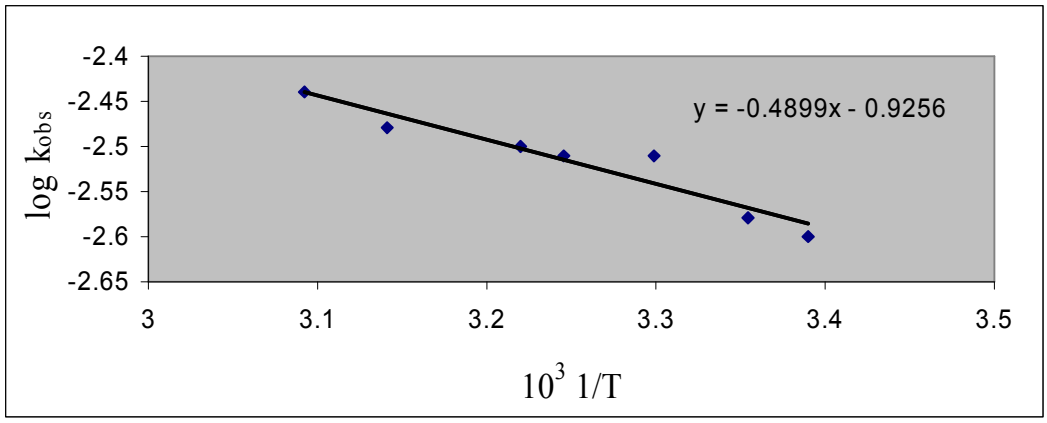

Figaer B11. Arrhenius plot for the aquation of 5-methyl-FFH in 25% by volume ethanol.

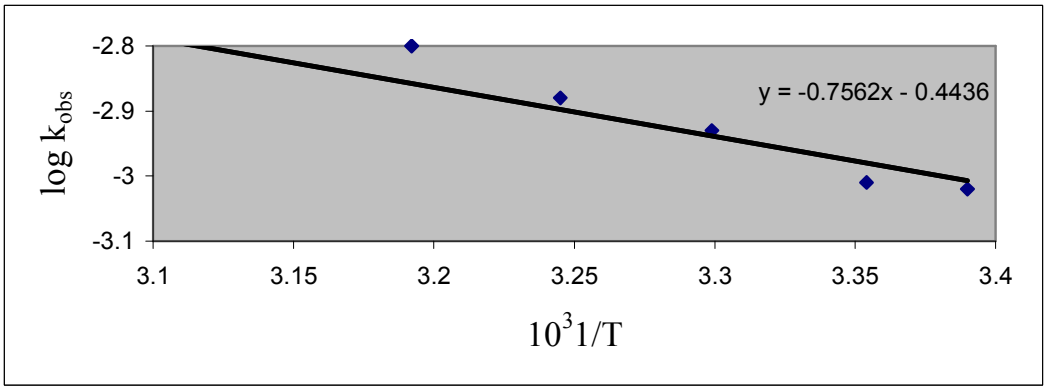

Figaer B12. Arrhenius plot for the aquation of 5-nitro-FFH in 25% by volume ethanol.

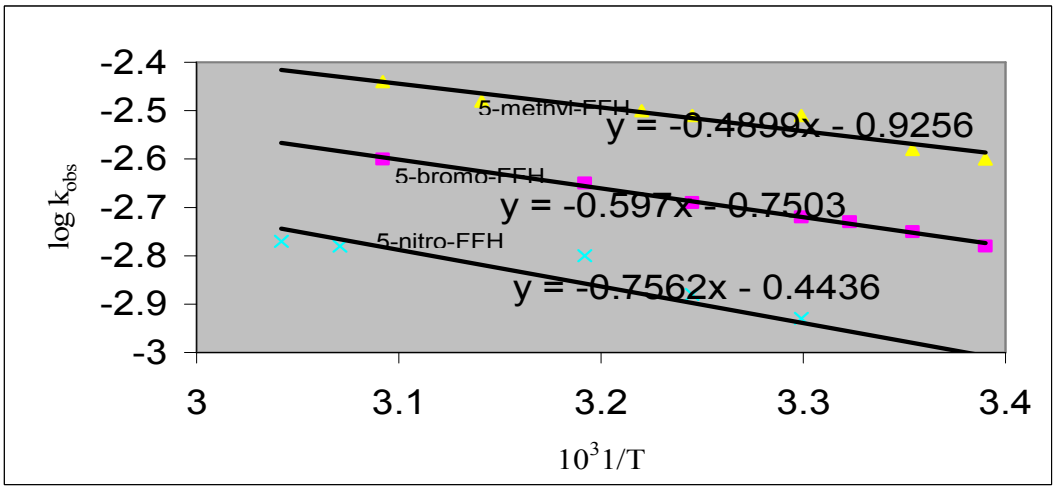

Figaer B13. Arrhenius plot for the aquation of FFH derivatives in 25% by volume ethanol

Table B8. Observed rate constants, activation energies and thermodynamic parameters of activation for the hydrolysis of 40 ppm hydrazones at pH 1.0, and room temperature 298.15K.

Compound	**$10^3 \cdot k_{obs} s^{-1}$**	**E_a kJ/mol**	**$\Delta H^{\neq}$ kJ/mol**	**$\Delta G^{\neq}$ kJ/mol**	**$\Delta S^{\neq}$ J/mol.K**
5-methyl FFH	2.63	9.38	6.90	84.42	-260.39
5-bromo FFH	1.80	11.49	9.01	83.44	-244.92
FFH	2.10	11.83	9.35	81.47	-242.14
5-nitro FFH	0.97	14.55	12.07	80.59	-232.26

Increase in the electron donating character of the substituents increase the electron density on the nitrogen atom of the azomethine linkage, which in turn causes a shift in the equilibrium to the products side.

Table B9. Average first order rate constants at different pH values for the aquation of FFH in acidic mediam at room temperature (298.15ºK)

pH	**$10^3.k_{obs}.s^{-1}$**	**log k_{obs}**
1.27	1.67	-2.78
1.39	1.30	-2.89
1.46	1.05	-2.98
1.59	0.83	-3.08
1.64	0.77	-3.11
2.00	0.25	-3.60

Table B10. Average first order rate constants at different pH values for the aquation of 5-nitro-FFH in acidic medium at room temperature

pH	**104.kobs**	**log kobs**
0.90	9.52	-3.02
1.17	4.76	-3.32
1.33	2.22	-3.65
1.43	1.93	-3.71
1.60	1.00	-4.00

Table B11. Average first order rate constants at different pH values for the aquation of 5-bromo-FFH in acidic medium at room temperature

pH	103.kobs.s-1	log kobs
1.00	0.88	-3.06
1.13	0.58	-3.24
1.25	0.36	-3.44
1.50	0.17	-3.77
1.67	0.12	-3.92
1.94	0.05	-4.30
2.05	0.04	-4.40

Table B12. Average first order rate constants at different pH values for the aquation of 5-methyl-FFH in acidic medium at room temperature

103.kobs.s-1	pH	log kobs
1.10	2.27	-2.64
1.18	2.07	-2.68
1.25	1.70	-2.77
1.60	0.56	-3.25
2.03	0.21	-3.68

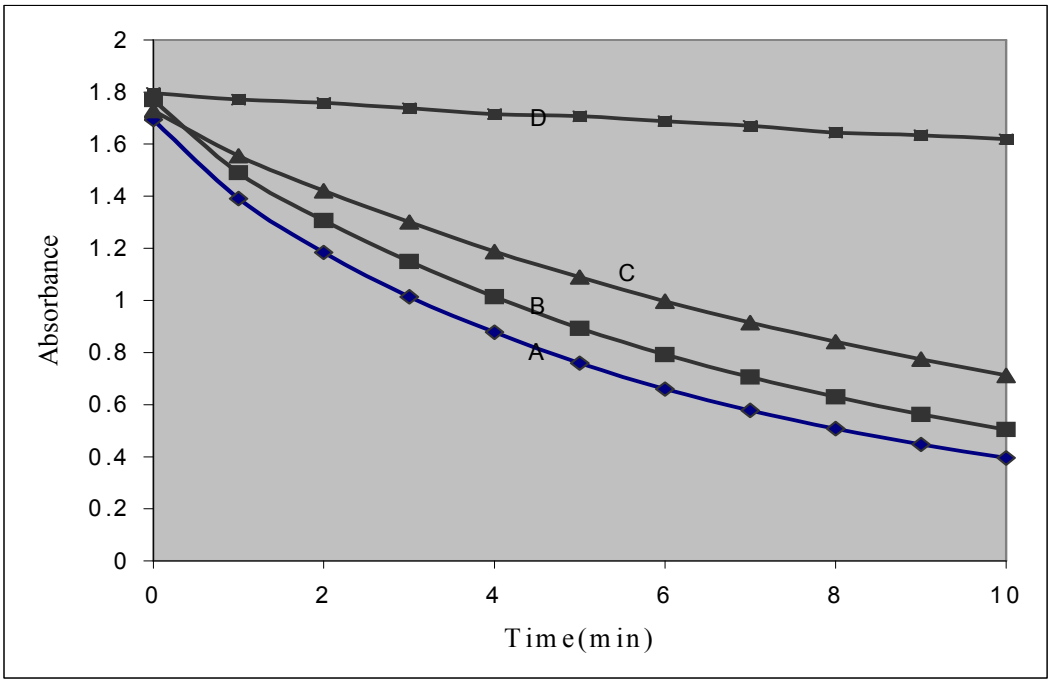

Figaer B14. A plot of absorbance versus time for the hydrolysis of 5-Methyl-FFH at different pH values (A: pH =1.10, B: pH =1.25, C: pH=1.60 and D: pH=2.03)

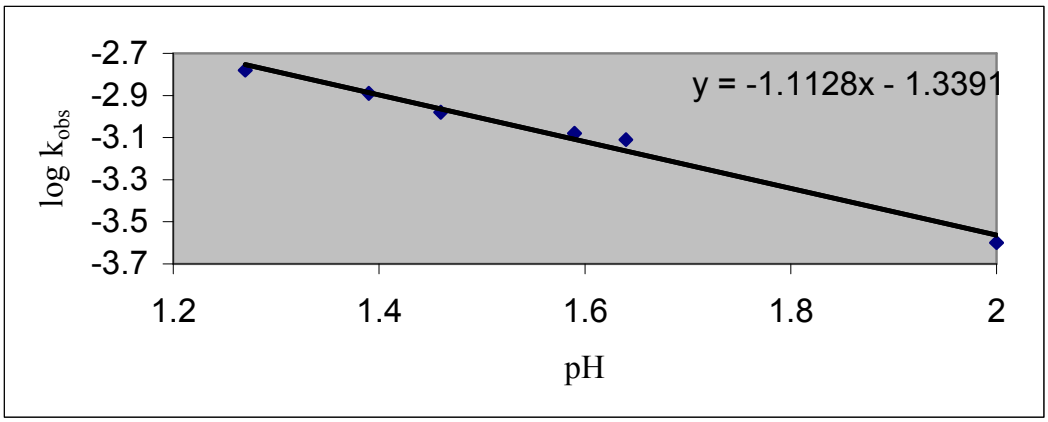

Figaer B15. A plot of log kobs versus pH for aquation of FFH in 25% ethanol(v/v) at room temperature

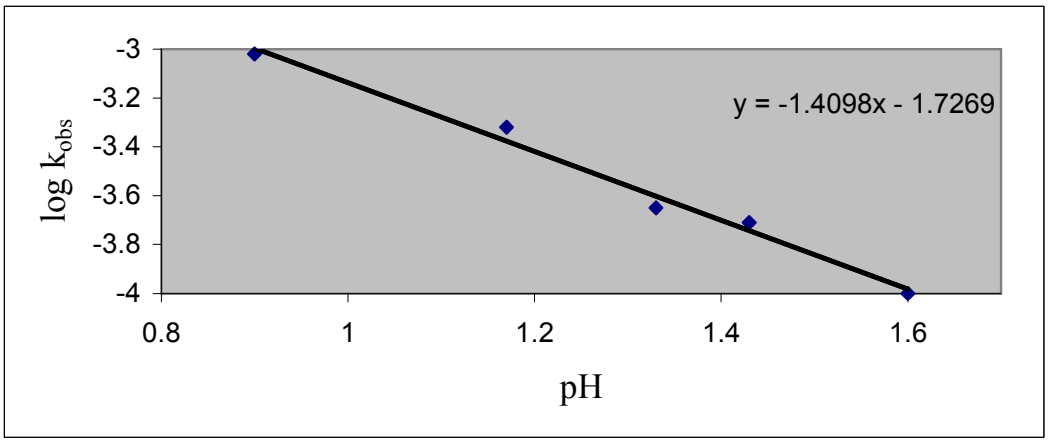

Figaer B16. A plot of log kobs versus pH for aquation of 5-nitro-FFH in 25% ethanol(v/v)at room temperature 298.15K

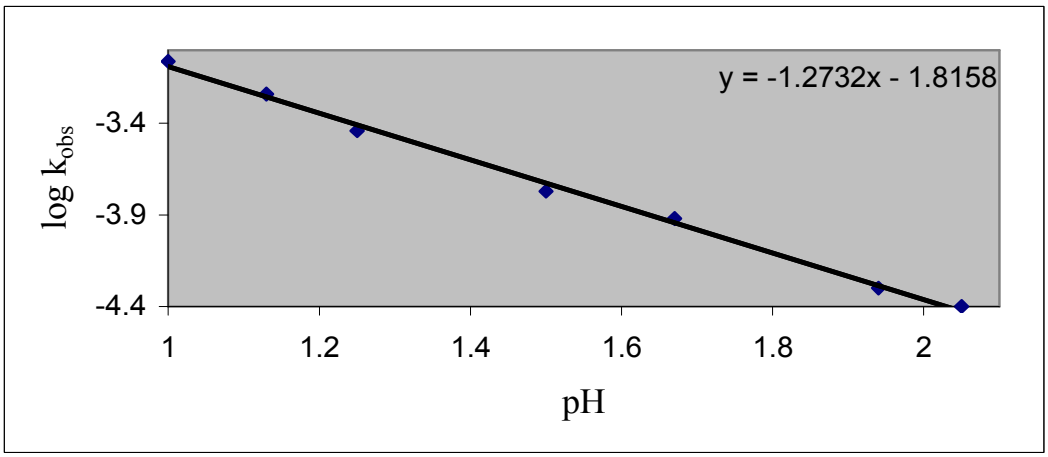

Figaer B17. A plot of log kobs versus pH for aquation of 5-bromo-FFH in 25% ethanol(v/v) at room temperature.

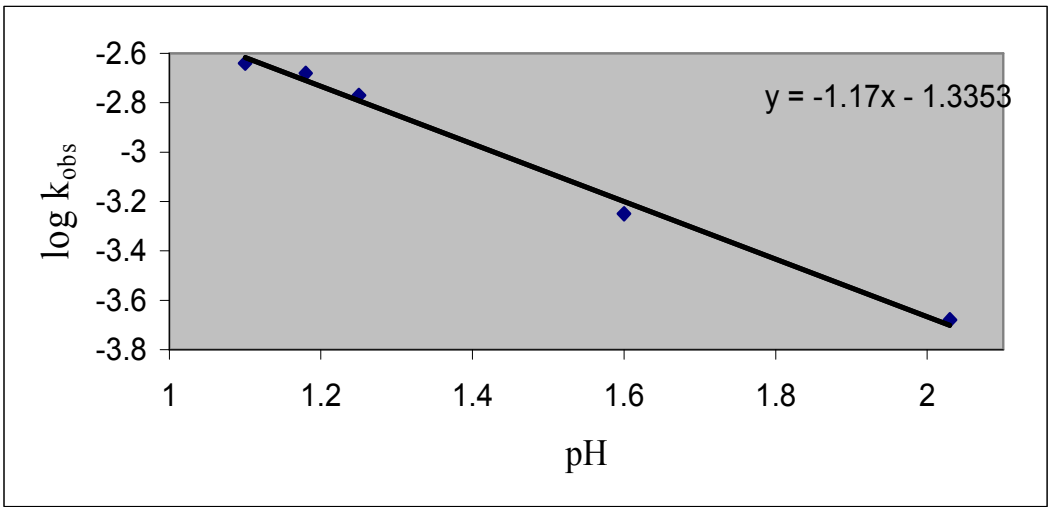

Figaer B18. A plot of log kobs versus pH for aquation of 5-methyl- FFH in 25 ethanol (v/v) at room temperature.

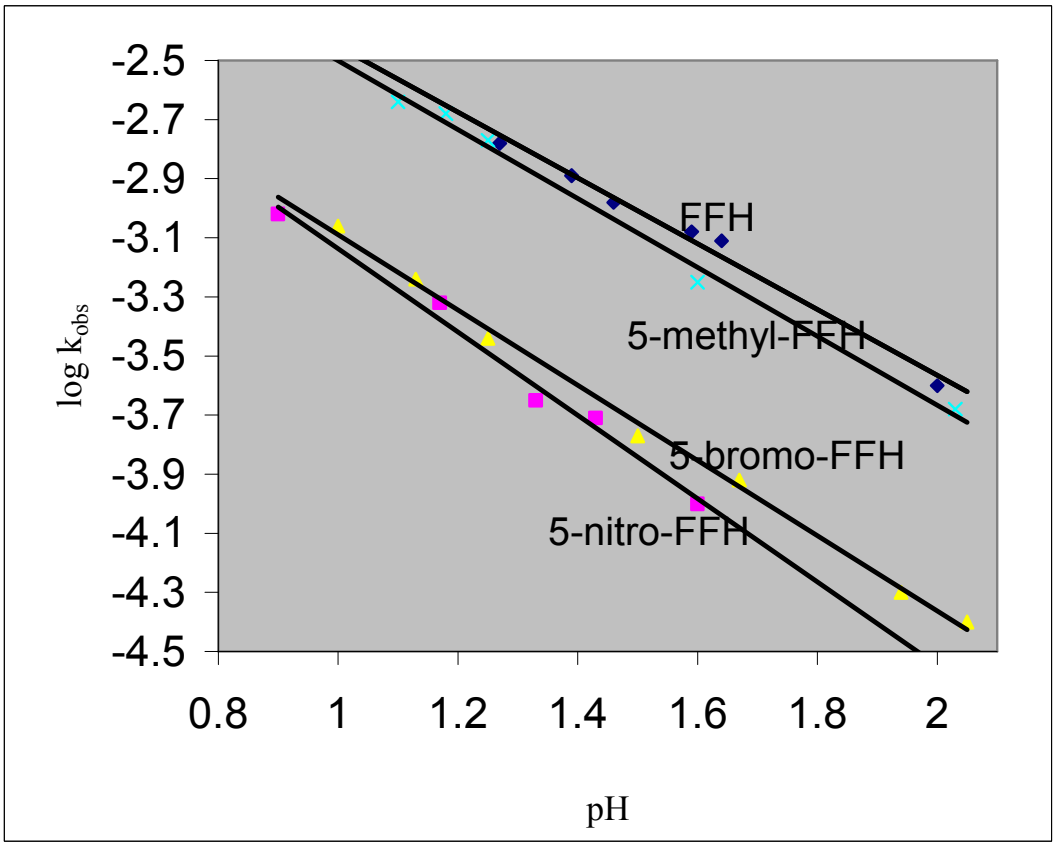

Figaer B19. A plot of log k_{obs} versus pH for aquation of FFH derivatives in 25% ethanol(v/v) at room temperature.

The mechanism of the reaction

From the above results the following mechanism is postulated.

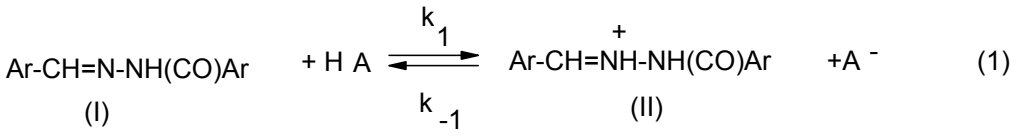

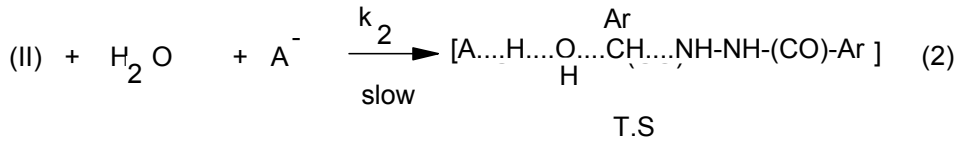

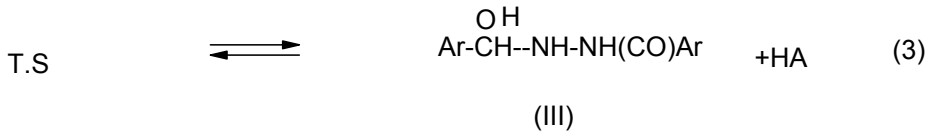

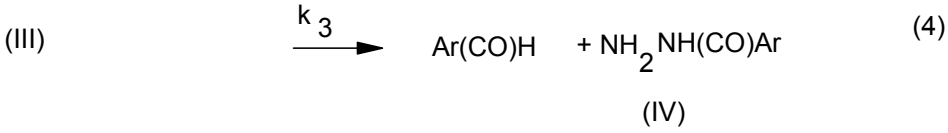

The rate of the reaction is the rate of the slowest step (step 2). Therfore,

Rate = k_2 [II][A^{-1}] where II means the protonated hydrazone

From step 1

K =[II] [A^{-1}] /([I][HA]) then

[II] = K[I][HA]/[A^{-1}]

Substituting the value of II gives

Rate = k_2 K[I]([HA]/[A^{-1}])[A^{-1}]

In each run the value of $[HA]/[A^{-1}]$ is kept constant denoted by **C**. Therefore the rate would be

$$Rate = k_2K\mathbf{C}[A^-][I]$$

This confirms with the general acid mechanism, since as the anion $[A^-]$ increase, the rate increase. Further more since the concentration of A^- is in much excess over the hydrazone (I). Therefore this will yield:

$$Rate = k [I]$$

Where k is the pseudo first order rate constant and equal to

$$k = k_2 K\mathbf{C}[A^-]$$

This mechanism is confirm exactly with the experimental findings as seen above.

The rate determining step is considered to be attack of water on the protonated hydrazide (step 2). This is supported by the finding that the observed rate constant increases with increasing electron donating group on the heterocyclic five member ring.

This intermediate (III) must undergo at least one proton transfer before decomposition to products, and such a proton transfer is expected to be fast.

If the reaction is subject to general acid-base catalysis then the following equation is obeyed

$$K_{obs} = k_0 + k_{HA}[HA] + k_{A^-}[A^-]$$

k_0 : The intrcept with Y axis

Now if the ratio $[HA]/[A^{-1}]$ is a constant value denoted by **x** then

$K_{obs}= k_0 +(k_{HA}+k_A^{-1}/x)[HA]$

A plot of k_{obs} versus [HA] will yield a straight line of slope = $k_{HA}+k_A^{-1}/x$ and an intercept of k_0.

Such plots are shown for the substituted methyl and bromo hydrazones in Figures B(17-19), the k_0 values ilustrated in Table B14.

Determination of the catalytic coefficients

Consulting Table B13, it is clear that $[HA/A^-]$ at pH = 0.60 is equal to 4.0 while $[HA/A^-]$ at pH =0.82 is equal to 2.5.

The slopes of the plots FigaerB(20-21) at these two differents pH are:

S_1 (pH=0.60) $=1.11x10^{-2}$

S_2 (pH=0.82) $=0.84x10^{-2}$

Then we have the following **2** equations

$1.11x10^{-2} = k_{HA} +k_A^-/2.5$

$0.84x10^{-2} = k_{HA} +k_A^-/4.0$

Using these two equations get

$k_A^- = 1.80x10^{-3}s^{-1}$

$k_{HA} =10.38x10^{-3}s^{-1}$

Calculation of k_{obs}

Now at pH =0.60 the intercept of FigaerB20 $= k_0 = 4.18x10^{-4}$, and [HA]= $3.0x10^{-3}$ M, $[A^-]=7.5x10^{-3}$M

Now substitutive in the equation

$K_{cal}= k_0 +k_{HA}[HA]+k_A^{-1}[A^{-1}]$

$= 4.18x10^{-4} + 10.38x10^{-3}[30.0x10^{-3}] +1.80x10^{-3}[7.5x10^{-3}]$

$= 7.63x10^{-4}s^{-1}$

The experimental value of k_{obs} as shown in Table B13 is 7.50×10^{-4} which shows excellent agreement with the calculated value.

Table B13. Effect of anion concentration of buffer on the observed rate constant for the hydrolysis of 5-methyl-FFH and 5-bromo-FFH at 25ºC

pH	10^3.[HA]	10^3.[A^-]	$10^4.k_{obs.}$ s^{-1}		$10^4.k_{cal}$ s^{-1}	
			5-methyl-FFH	5-bromo-FFH	5-methyl-FFH	5-bromo-FFH
0.6 0	30.00	7.50	7.50	2.94	7.43	2.58
	56.24	14.06	10.42	4.33	10.27	4.00
	75.00	18.75	12.49	5.36	12.30	5.10
	----------	----------	----------	---------	----------	---------
0.82	18.75	7.50	4.54	2.00	3.40	1.96
	37.50	15.00	7.20	3.28	5.48	3.13
	56.25	22.50	8.10	3.99	7.56	4.20
	75.00	30.00	9.46	5.62	9.64	5.45

Table B14. Variation of the observed rate constant for the hydrolysis of FFH derivatives at zero buffer concentration at room temperature

pH	k0	
	5-Methyl-FFH	5-Bromo-FFH
0.60	$4.18x10^{-4}$	1.32×10^{-4}
0.82	$3.41x10^{-4}$	0.83×10^{-4}

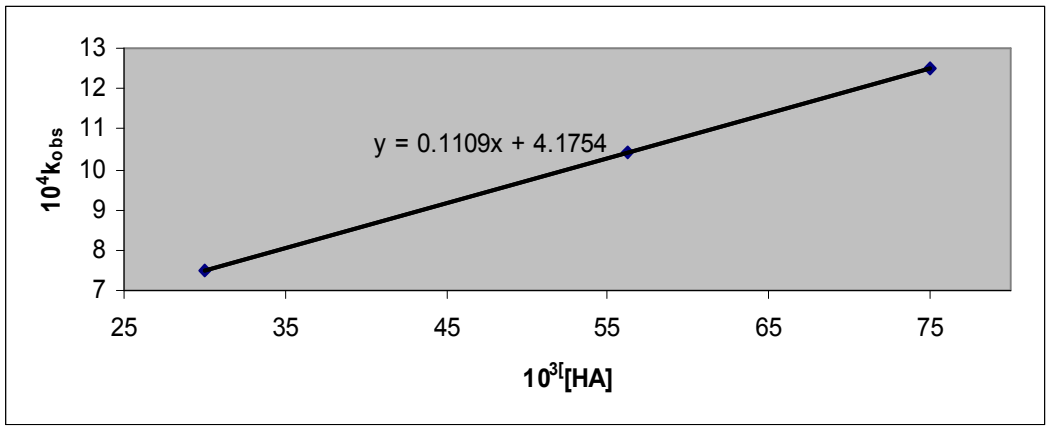

Figaer B20. A plot of [HA] versus k_{obs} for the hydrolysis of 5-methyl-FFH at pH =0.60 and [HA]/[A] = 4.0

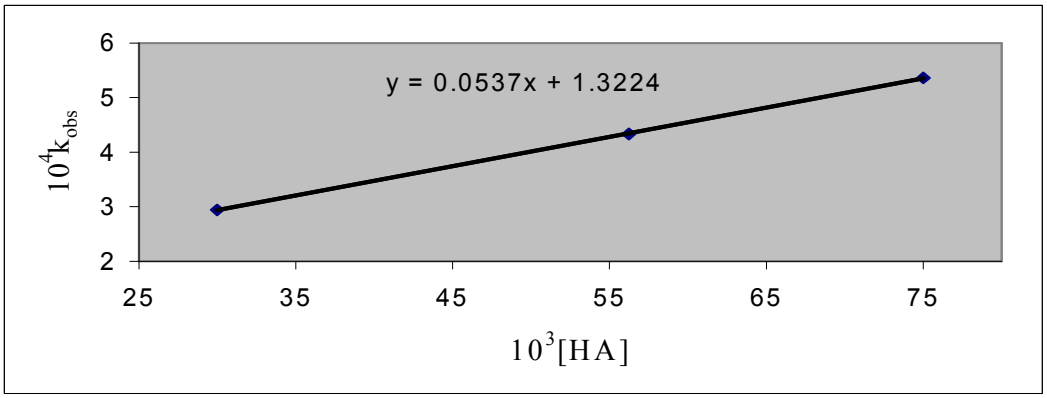

Figaer B21. A plot of [HA] versus kobs for the hydrolysis of 5-bromo-FFH at pH =0.82 and [HA]/[A] =2.5

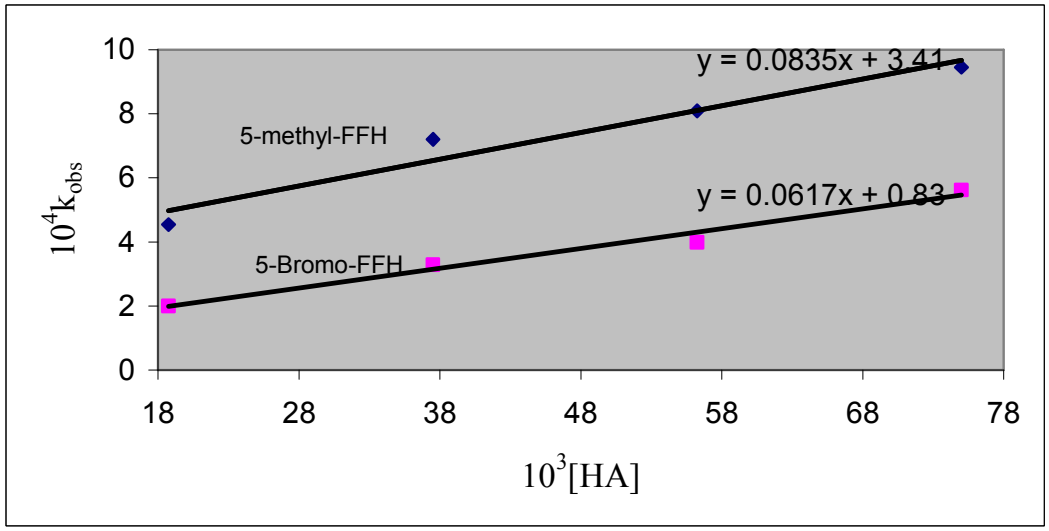

Figaer B22. A plot of [HA] versus kobs for the hydrolysis of 5-bromo-FFH and 5-methyl-FFH at pH =0.82 and [HA]/[A] = 2.5

Plotting k_0 versus $[H^+]$ we have got a straight line with a slope equal to k_H^+ according to the equation :

$$k_0 = k_{uncat} + k_H^+[H^+]$$

Nowing that k_{uncat} has very low value and thus can be ignored then $k_0 = k_H^+[H^+]$

Therefore, the observed first order rate constant for the hydrolysis of 5-methyl-FFH in oxalic acid –tetraoxalate buffer at room temperature can be expressed by the following equation:

$$k_{obs} = 1.60x10^{-4}[H^+] + 8.67x10^{-3}[HA] + 5.33x10^{-3}[A^{-1}]$$

The observed first order rate constant for the hydrolysis of 5-bromo-FFH in oxalic acid –tetraoxalate buffers at room temperature can be expressed by the following equation:

$$k_{obs} = 7.00x10^{-4}[H^+] + 4.6x10^{3}[HA] + 4.0x10^{-3}[A^-]$$

The linear correlation between the activation enthalpies and entropies FigaerB23 implies that all the hydrazone derivatives are hydrolysed by the same mechanism and the changes in the rates are governed by the changes in both enthalpies and entropies of activation FigaerB23.

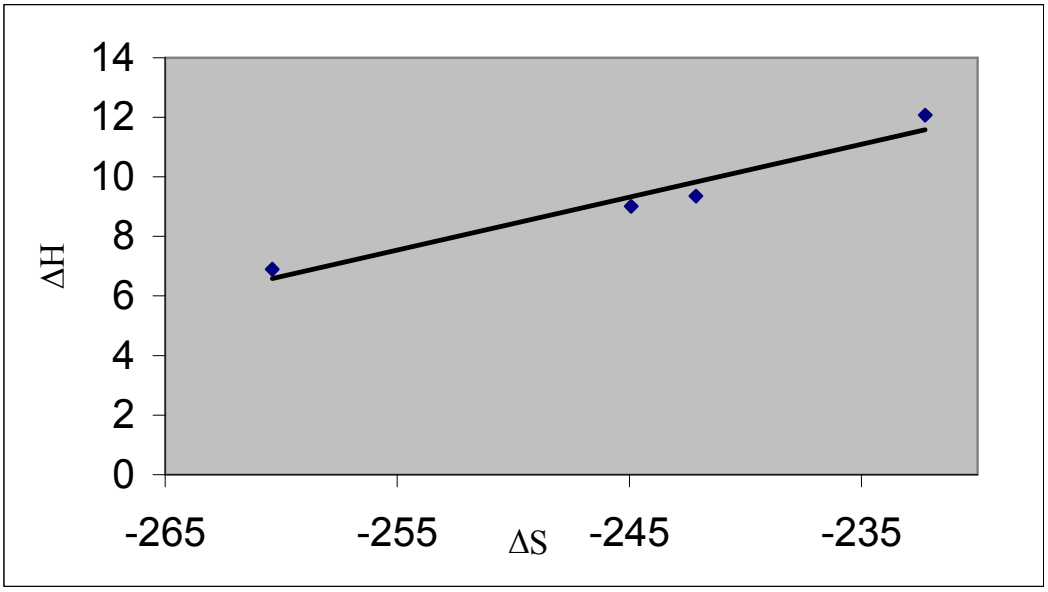

Figaer B23. A plot of Δ H≠(kJ/mol) versus ΔS≠(J/mol. K) for X-FFH at room temperature and pH 1.0

Part C: Fluorescence

Fluorescence spectra

H_2O_2 oxidises di-2-pyridylketonebenzoyl hydrazone (DPKBH) in acidic medium to produce a fluorescent product. Excitation and emission wavelengths for the fluorescent product illustrated in FigaerC1

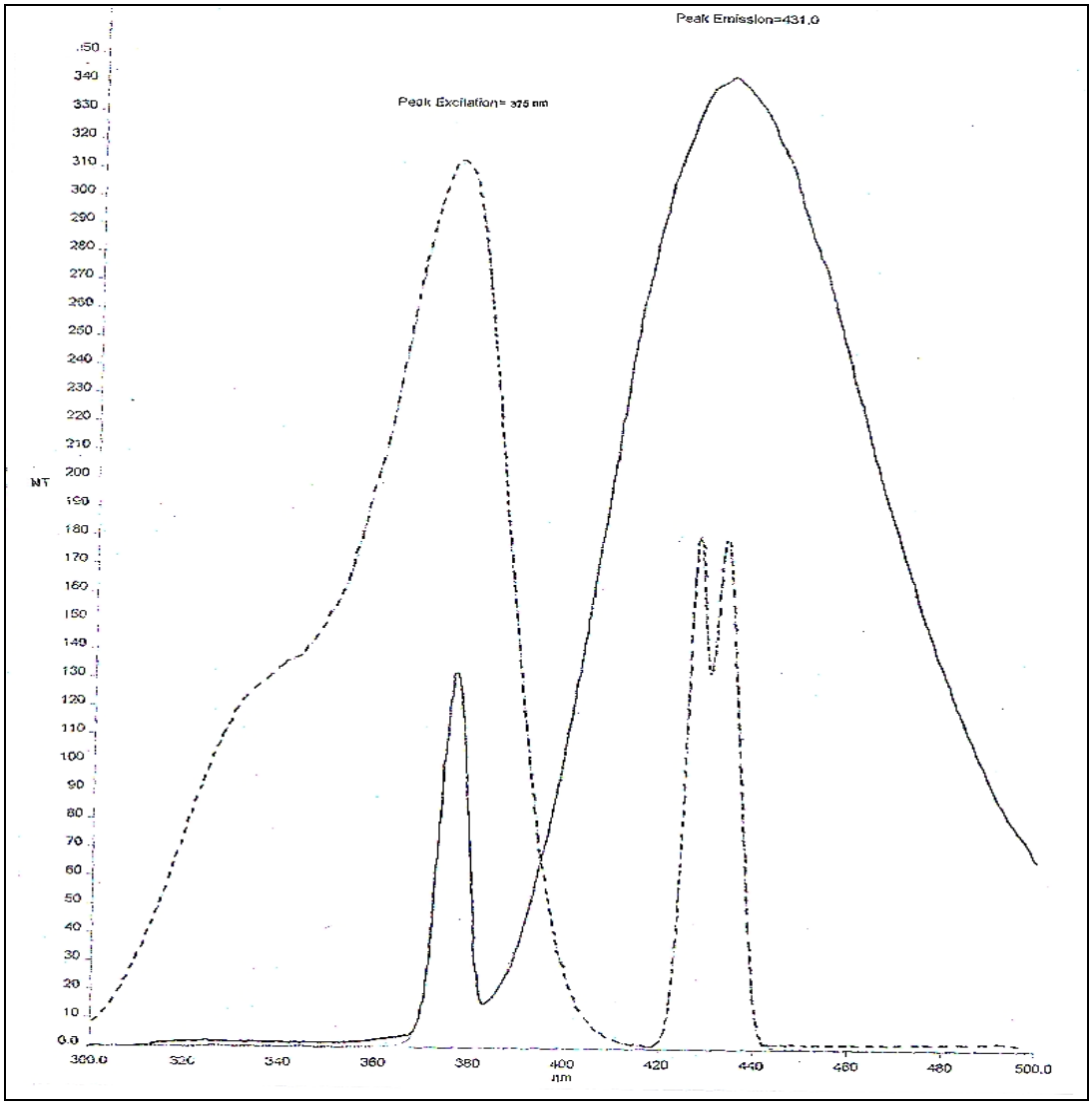

Figaer C1. Fluorescence spectra of the oxidative product of DPKBH, $[H_2O_2]$= 7.0%, [HCl] = 4M, [DPKBH] = $4.67x10^{-5}$M and [Fe(III)] = $1.56x10^{-5}$M

Effect of pH

The effect of pH on the system was studied using different concentration of HCl. The optimum pH was found to be 4M HCl working solution as shown clearly in FigaerC2

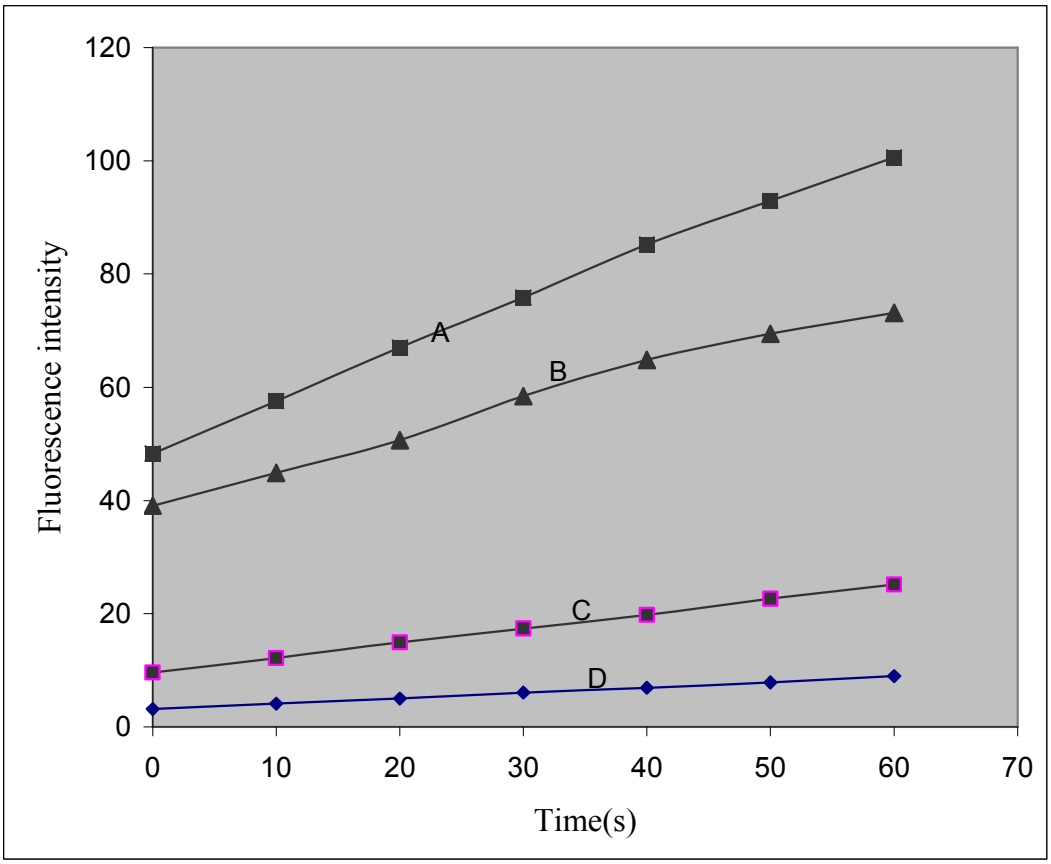

Figaer C2. A plot of fluorescence intensity versus time at different concentrations of HCl for the oxidative product of DPKBH, $[H_2O_2]$=7%(v/v), [DPKBH]= $4.67x10^{-5}$M, (A: [HCl]=4M, B: [HCl]=3.5M, C:[HCl]=2.5M and D: [HCl]=2M).

Effect of hydrogen peroxide

The effect of H_2O_2 was studied using different concentration of H_2O_2 from (1.2 to 7.0%). It was observed that H_2O_2 has no effect on the rate of reaction, which means that the reaction is zero order with respect to H_2O_2. The result is shown in Table C1

Table C1. Fluorescence intensity versus time for the oxidative product of DPKBH, using different percentage of H_2O_2, [HCl]= 4M and [DPKBH]= $4.67x10^{-5}$M.

Time (sec)	H2O2				
	1.20%	**1.70%**	**3.50%**	**5.20%**	**7.00%**
0	54.31	53.53	56.64	57.13	54.72
10	57.73	56.01	59.36	60.38	57.68
20	60.22	58.39	61.5	63.03	60.47
30	62.85	60.71	63.7	65.18	62.59
40	65.12	62.8	65.5	67.92	65.35
50	67.52	65.06	67.42	70.09	66.99
60	69.52	67.17	69.2	72.87	69.41

Effect of DPKBH Concentration

Increasing the concentration of DPKBH results in increasing the rate of reaction. The results are shown in Table C2, and so in all results the concentration of hydrazone used corresponded to $4.67x10^{-5}$M.

Table C2. Fluorescence intensity at different time of the oxidative product for DPKBH, using different [DPKBH], [HCl] =4M and H_2O_2 = 7%(v/v)

	105[DPKBH]/mol/liter				
Time(s)	**4.67**	**4.20**	**3.34**	**1.40**	**0.93**
0	71.51	58.38	52.15	43.83	35.71
10	92.23	76.01	65.05	54.01	43.45
20	110.45	90.82	75.08	62.03	49.70
30	126.25	103.4	84.14	69.79	54.55
40	138.57	112.59	92.61	75.24	59.19
50	149.42	122.32	102.33	81.48	66.3
60	160.21	133.34	112.61	91.12	72.61

Effect of iron

Addition of iron(III) to the hydrazone decreases the rate of thereaction. It was found that, there was a linear relationship between the

emitted fluorescence intensity and Fe(III) concentration up to $3.0x10^{-6}$M of Fe (III). The result is shown in Table C4 and is illustrated in FigaerC3

Table C3. Variation of fluorescence intensity for the oxidative product of DPKBH at different concentration of Fe(III), [HCl]=4M, H2O2= 7%(v/v) and 4.67x10-5M DPKBH after 50s

10^{-5}.[Fe(III)]	F.Intensity (after 50 sec)
0.00	70.1 7
0.17	70.19
0.25	70.78
1.06	66.93
2.46	64.10
3.17	60.00
7.04	55.67
10.60	50.00
14.10	44.50
17.60	39.16
21.00	37.01
24.00	33.02
28.20	29.21
31.70	24.83
35.20	18.58

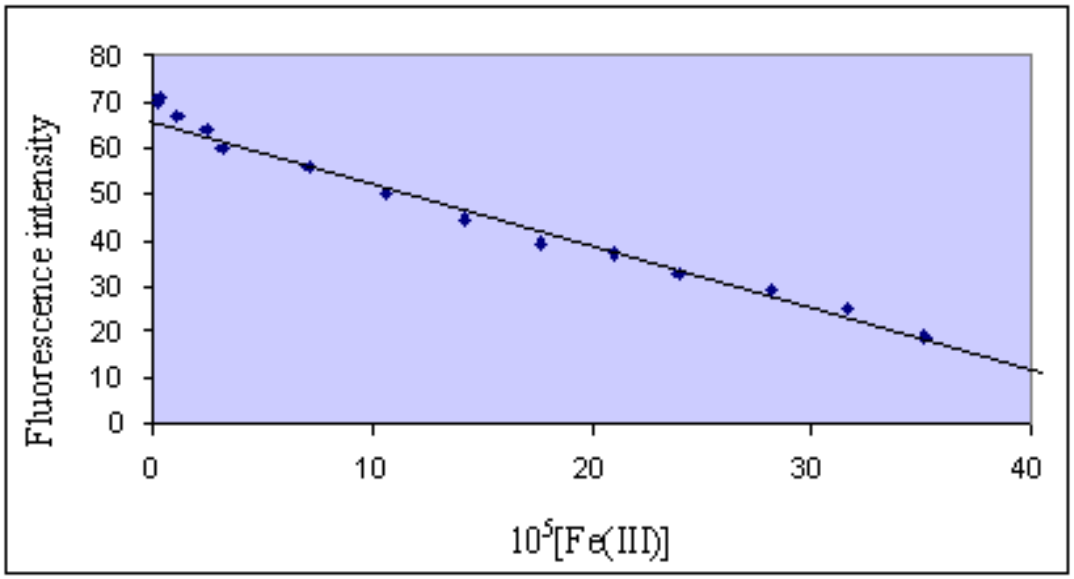

Figaer C3. A plot of fluorescence intensity after 50s of the oxidative product against [Fe(III)]. [HCl]= 4M, [H2O2] = 7%(v/v) and [DPKBH] = 4.67x10-5M.

Order of additions

The best order of addition the reagent that gives the most reproducible results is as follows iron(III), DPKBH, HCl and H_2O_2.

Reproducibility

Analysis of ten replicates showed that the results are reproducible with a relative standard deviation (RSD)of 4.03% for rate and 3.08% for intensity (after 50 s), these results are shown in Table C4.

Table C4. Reproducibility data for the oxidative product of DPKBH by H2O2 in acidic medium, [HCl] =4M, [DPKBH] =4.67x10-5M and 7.0% (v/v) H2O2

%Fe(III)/DPKBH	Fluorescence intensity(after 50 s)
0.00	31.20
0.28	28.22
0.56	25.28
0.85	22.49
1.12	19.70
1.58	19.55
1.78	19.63
1.96	19.67

Stoichiometric study

The fluorescence intensity or rate decreases until the ratio of [Fe(III)]/ [DPKBH] is nearly unity. This result showed that upon addition of Fe(III) to hydrazone a 1:1 complex is formed. The result is shown in FigaerC4, and table C5. The complex formation of the hydrazone with Fe(III) is believed to occur since a change of colour to yellowish green is observed when Fe(III) is added to the solution.

Table C5. Fluorescence intensity after 50 s for the oxidative product of DPKBH at different percentage of Fe(III)/DPKBH

Run number	F.Intensity(after 50 s)	Rate.s-1
1	64.40	0.64
2	62.80	0.65
3	61.23	0.60
4	65.65	0.68
5	64.11	0.65
6	67.74	0.66
7	65.64	0.60
8	61.45	0.62
9	63.81	0.63
10	64.21	0.65

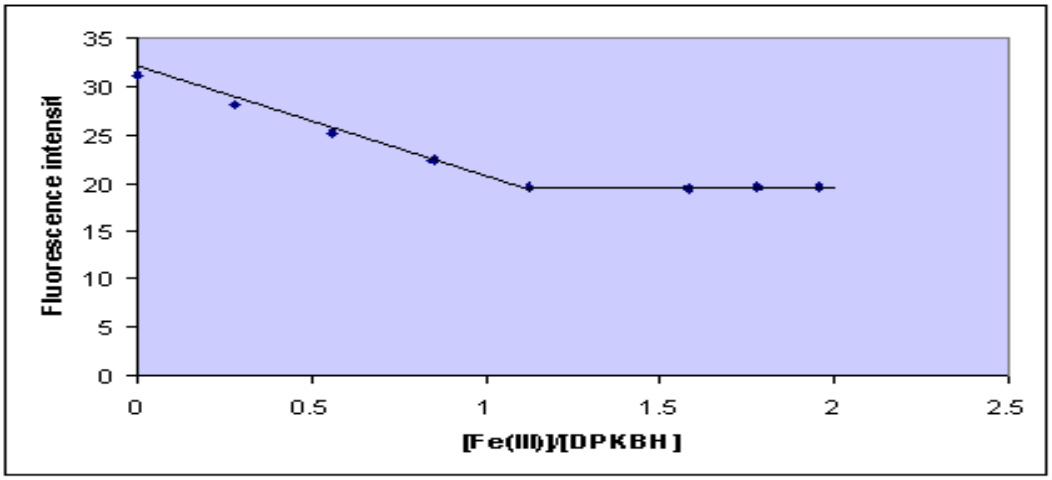

Figaer C4. A plot of fluorescence intensity after 50 s of the oxidative product against [Fe(III)]/[DPKBH]. [HCl] = 4M and [H2O2] = 7% (v/v).

Interference study

There are a number of ways in which chemical species might interfere with this method :

a- species decreasing the actual concentration of hydrazone via complexation or oxidation.

b- metal complexing agents.

c- specieses affect the pH value of solution.

By an identical technique to that used for the determination of iron, the effects of 20 ions on the proposed method were examined. The effect of such species on the determination of $1.56x10^{-5}$ M of Fe(III) was investigated by first testing a 100 fold (mol/mol) ratio of foriegn ions. If interference occurred, the ratio reduced until no interference. The results are showed in table C6. The results show that this method suffers from lack of interference except copper (II) which will be tolerated up to 11.5 fold and iodide ion up to 15 fold.

Table C6. Interference of some ions effect to the fluorescence intensity and initial rate in precence of iron ions

Foreign ion	**Salt**	**Cion/CFe(III)**
Sr(II)	$Sr(NO_3)_2$	100
Ba(II)	$Ba(NO_3)_2$	100
Mn(II)	$Mn(NO_3)_2$	100
Ag(I)	$AgNO_3$	100
Pb(II)	$Pb(NO_3)_2$	100
Cr(III)	$Cr(NO_3)_3$	65
K(I)	KNO_3	100
Al(III)	$Al(NO_3)_3$	100
Cu(II)	$Cu(NO_3)_2$	11.5
Bi(II)	$Bi(NO_3)_2$	50
Na(I)	$NaNO_3$	100
Sn(II)	$Sn(NO_3)_2$	50
Zn(II)	$Zn(NO_3)_2$	100
Co(II)	$CoCl_2$	100
SO_4^{-2}	Na_2SO_4	100
I^-	KI	15
ClO_3^-	$KClO_3$	100
Br^{-1}	KBr	56
NO_3^-	KNO_3	100
Cl^-	$CoCl_2$	100

Applications

The described method was applied to the determination of iron in several samples of medicines and milk. From the calibration graph FigaerC3, the amounts of iron in the samples are calculated as shown in Table C7.

Table C7. The amount of iron in analyte sample calculated

$[Fe]_{actual}$	Sample	% Error	$[Fe]_{found}$
50mg/ml	Ferrilet-3	1.68	49.16mg/ml
10mg/100g	Milk	1.00	9.90mg/100g

References

Abu-Baker. M.El-Nady: S**pectrophotometric and polographic studies on the kinetics of hydrolysis of N-(6- methyl-5- nitropyridin-2- yl methyllidene) -N-(thiazol-2-yl) hydrazones**, J. Chin.Chem. Soc, 48(6B), (2001), 1081-1086.

Abu-Eid. M.A., Abu-Zuhri. A.Z, Mahmoud. F.M and Shraydeh. B.F: **Kinetics and mechanism of the hydrolysis of benzylidene benzoyl hydrazone derivatives**, An-Najah. J. Res, I(6), (1989), 23-34.

Abu-Zuhri. A.Z, Abu-Eid. M.A, Al-Nuri. M.A. and Mahmoud. F.M: **Kinetic studies on the hydrolysis of pyrrolidene benzoyl hydrazone and thiophenylidene benzoylhydrazone,** J.Fac. Sci. U.A.E.Univ, 4 (1992).

Brown. C.J and Kirby. A.J: **General acid base catalysis mechanism**, J. Chem. Soc, Perkin Trans, 2, (1997), 1081-1093.

Degtyarenko. K.M, Kopylova. T.N, Kuznetsova. R.T, Mayer. G.V and Tel'minov.E.N: **The effect of H-bonding solvents on the electronically excited states properties of 7-dimethyl amino-4-methyl-coumarin and psoralens,** Atmos. Oceanic Opt., 6, (1993), 421-428.

Frankel. L.S, Langford.C. H and Stengle.T.R: **Preferential solvation**, J.Phys.Chem, 74(6), (1970), 1376-1381.

George. G.G: Fluorescence spectrum, **Practical fluorescence, 2thEdit**, (1990), 10-14.

Henry. H.B, Gary. D and James. E.O: I**ntroduction to spectroscopic methods**, Instrumental Analysis, 1st Edit, (1978), 139-153.

Hering. J.G, Morel. F.M.M: **Introduction to spectrofluoremetric determination of elements**, J. Envirron.Sci. Technol, 24, (1990), 242-252.

Jinzhang. G.A.O, Jianniao. T.I.A, Yanchun. Z.H.A, Wu.Y.A.N and Hualing.D.E.N: **Spectrofluorimetric determination of gallium with calon-carboxylic acid**, Rare metals, 22(1), (2003), 123-129.

Jong. P.L and Tae-Seop. U: **Kinetics and Mechanism of the Hydrolysis Reaction of N-Furoyl-2-phenylimidazole**, Bull. Korean Chem.Soc, 21(129), (2000), 604-614.

Karvinen. J, Laitala. V, Makinen. M.L, Mulari. O, Tamminen. J, Hermonen.J, Hurskainen.P and Hemmila.I: F**luorescence quenching based assays for hydrolyzing enzymes.** Application of time resolved fluorometry in assays for caspase, helicase and phosphatase. J.Anal.Chem, 76, (2004), 1429-1436.

Khashaba. P.Y: **Spectrofluorimetric analysis of certain macrolide antibiotics in bulk and pharmaceutical formulations**, J.Metadata search: Elsevier.J.Pharmaceutical and Biomedical Analysis, 27(6), (2002), 923-932.

Kurokawa. Y. ; Maekawa. A, Takahashi M, Hayashi.Y: **Toxicity and carcinogenicity of potassium bromate a new renal carcinogen**, Environmental Health Perspectives, 87, (2001), 309-335.

Laidler.K.J, Meiser.J.H and Sanctuary.B.C: **Specific acid base catalysis**, Physical Chemistry,4^{rth} edition, (2003), 451-453.

Lin. C.F, Lee. D.Y, Chen.W.T and Lo.K.S: **Spectrofluorimetric Analysis,** J.Environ. Pollut, 87, (1995), 181-187.

Mak. M.K, Langford.C.H: **Fluorescence quenching,** Can.J.Chem, 60, (1982), 2023-2028.

Mark. L.D and Lond.F.F: First order reactions. **Introduction to physical chemistry**, 3rd Edition, 1998, 416-417.

Neeley. W.E, Cupas. C.A: **The use of 3-methyl-2-benzothiazolone hydrazone in clinical chemistry: a convenient micromethod for the determination of serum or plasma glucose**, J.Clin.Bio.Chem, 6(4), (1973), 246-455.

Nevado. J.J.B, Pulgarh. J.A.M and Laguna. M.A.G: **Spectrofluorimetric determination of vitamin k_3**, J. Analyst,123(2), (1998), 287-290.

Oshite. S, Furukawa.M and Igarashi.S: **Homogeneous liquid-liquid extraction method for the selective spectrofluorimetric determination of trace amounts of tryptophan**, J. Analyst, 126(5), (2001), 703-706.

Ren. J.L, Zhang. J, Luo. J.Q, Pei. X.K and Jiang. Z.X: **Improved fluorimetric determination of dissolved aluminium by micelle – enhanceed lumogallion complex in natural waters**. J.Analyst, 126(5), (2001), 698-702.

Rigler. R and Elson. E.S: Eds. **Fluorescence Correlation Spectroscopy: Theory and Application**; Springer-Verlag: Berlin, 1st Edit, (2001). 152-158.

Robert. D.B: (1983), **Fluorescence analysis**, Introduction to chemical analysis, 1st Edit, 203-206.

Robert. K.E, Lloyd and Clarke. D.J: **Sensitively and specificityenhancement in fluorescent analysis**, J. Pharmacy and Pharmacology, 54, (2002), 9-15.

Rubio. S, Gomez-Hens.A and Valcarcel. M: **Analysis of binary and ternary mixtures of titanium, zirconium, and hafnium by**

derivative synchronous fluorescence spectrometry, J. Anal. Chem, 57(6), (2001), 1101-1106.

Shoeb. H.A, Bowman. B.U, Ottolenghi. A. C and Merola. A.J: **Peroxidase-mediated oxidation of isoniazid**, J.Antimicrob Agents Chemother, 27(3), (1985), 399-403.

Soukup. R.W and Schmid.R: **Solvent effects in organic chemistry**, J.Chem.Educ, 62(6), (1985), 459-461.

Tang. B, Du. M, Wang. Y, Zhang. X and Zhang. C, J: **Highly sensetive spectrofluorimetric determination of trase amounts of scandium with salicylaldehyde salicylhydrazone,** J.Analyst, 123(2), (1998), 283-286.

Tinoco. I, Sauer. K and Wang. J. C: **Temperature dependence**, Physical Chemistry: Principles and applications in biological Sciences, 3rd edition, (1995), 365-372.

Uno.T and Taniguchi. H: S**tudies on the hydrazone derivatives in fluorometric analysis. II.** Fluorometric determination of aluminum, J. Jap. Anal, 20(9), (1971), 1123-1128.

Wuilloud. R.G, Wuilloud. J. C, Olsina. R. A and Martenez. L. D: **Speciation and preconcentration of vanadium(V) and vanadium(IV) in water samples by flow injection inductivvely coupled plasma optical emission spectrometry and ultrasonic nebulization**, J.Analyst, 126(5), (2001), 715-719.

Yutaka. N, Yoshito.A and Tadashi.O: **Solvent dependent ultrafast ground state recovery dynamics of triphenyl methane dyes**, J. Chinese. Chem .Soc, 47(4A), (2000), 699-704.

جامعة النجاح الوطنية
كلية الدراسات العليا

دراسة ميكانيكية وحركة تفاعل التميؤ لسلسة من مشتقات غير فريلدين فيرويل هايدرازون، تأثير المذيبات على طاقة الامتصاص، استخدام ظاهرة الأطياف في تحليل الحديد عن طريق أكسدة مركب ثنائي −2− بيريديل كيتون بنزويل هايدرازون باستخدام مركب H_2O_2

إعداد
محمود محمد عيسى قباجة

إشراف
الدكتور باسم شريدة

قدمت هذه الأطروحة استكمالاً لمتطلبات درجة الماجستير في الكيمياء بكلية الدراسات العليا في جامعة النجاح الوطنية.في نابلس، فلسطين.

2005م

دراسة ميكانيكية وحركة تفاعل التميؤ لسلسة من مشتقات غير فريلدين فيرويل هايدرازون، تأثير المذيبات على طاقة الامتصاص، استخدام ظاهرة الأطياف في تحليل الحديد عن طريق أكسدة مركب ثنائي –2– بيريديل كيتون بنزويل هايدرازون باستخدام مركب H_2O_2

إعداد

محمود محمد عيسى قباجة

إشراف

الدكتور باسم شريدة

الملخص

كما لدراسة تأثير المذيبات المختلفة على طاقة الامتصاص لمركب ثنائي –2– بيريديل كيتون بنزويل هايدرازون في مذيب الماء ايثانول في درجة حرارة الغرفة.

كما قمنا بدارسة ميكانيكية وحركة تفاعل التميؤ لسلسة من مشتقات فيرفريليدين فيرويل هايدررازون بواسطة أطياف الأشعة فوق البنفسجية والمرئية، حيث وجدنا أن تفاعلات التميؤ تتبع حركة الرتبة الأولى، كما تم دراسة تأثير درجة الحموضة ودرجة الحرارة على سرعة التفاعل، ولقد فرضت ميكانيكية التفاعل التي تحتوي على هجموم جزئي الماء على الهدف والذي اعتبر كمساعد حامض–قاعدة عام باستخدام استيات الصوديوم –حمض الهيدروكلوريك، ولقد تم تقييم عوامل أرهينياس والعوامل الحرارية المختلفة.

تم استخدام ظاهرة الأطياف Fluorescence في تحليل الحديد الثلاثي عن طريق أكسدة مركب ثنائي –2– بيريديك كيتوك بنزويل هايدرازون باستخدام مركب H_2O_2 حيث وجد أن الحديد يعمل على تقليل انبعاث الطيف، ووجد ان أقل تركيز للحديد يمكن كشفه 3×10^{-6} مول/ليتر.

وتم دراسة تأثير الدقائق الغريبة الموجودة في المحلول، ولقد استخدمت الطريقة بنجاح في تحليل الحديد في الحليب والأدوية.